Yeast chaperone Hsp70-Ssb modulates a variety of protein-based heritable elements

Lina M. Jay-Garcia[1£], Joseph L. Cornell[1], Rebecca L. Howie[1¶], Quincy L. Faber[1#], Abigail Salas[1], Tatiana A. Chernova[2], and Yury O. Chernoff[1*]

[1]*School of Biological Sciences, Georgia Institute of Technology, Atlanta, GA 30332-2000, USA*

[2]*Department of Biochemistry, Emory University School of Medicine, Atlanta, GA 30322, USA*

[£]Present affiliation: National Center for Emerging and Zoonotic Infectious Diseases (NZEZID), Centers for Disease Control and Prevention, Atlanta, GA, USA

[¶]Present affiliation: Bacterial Meningitis Lab, Centers for Disease Control and Prevention, Atlanta, GA, USA

[#]Present affiliation: Microbiology and Cell Science Department, University of Florida, Gainesville, FL, USA

[*]Corresponding author. Mailing address: Roger A. and Helen B. Krone Engineered Biosystems Bldg., Georgia Institute of Technology, M/C 2000, 950 Atlantic Drive, Atlanta, GA 30332-2000, tel. 404-894-1157, fax 404-894-0519, cell 678-756-2234, E-mail yury.chernoff@biology.gatech.edu

Abstract:

Prions are transmissible self-perpetuating protein isoforms associated with diseases and heritable traits. Yeast prions and non-transmissible protein aggregates (mnemons) are frequently based on cross-β ordered fibrous aggregates (amyloids). Formation and propagation of yeast prions are controlled by the chaperone machinery. Ribosome-associated chaperone Hsp70-Ssb is known (and confirmed here) to modulate formation and propagation of the prion form of Sup35 protein, [*PSI*$^{+}$]. Our new data show that both formation and mitotic transmission of the stress-inducible prion form of Lsb2 protein, ([*LSB*$^{+}$]) are also significantly increased in the absence of Ssb. Notably, heat stress leads to a massive accumulation of [*LSB*$^{+}$] cells in the absence of Ssb, implicating Ssb as a major downregulator of the [*LSB*$^{+}$]-dependent memory of stress. Moreover, the aggregated form of Gγ subunit Ste18, [*STE*$^{+}$], behaving as a non-heritable mnemon in the WT strain, is generated more efficiently and becomes heritable in the absence of Ssb. Lack of Ssb also facilitates mitotic transmission, while lack of the Ssb cochaperone, Hsp40-Zuo1 facilitates both spontaneous formation and mitotic transmission of the Ure2 prion, [*URE3*]. These results demonstrate that Ssb is a general modulator of the cytosolic amyloid aggregation, whose effect is not restricted only to [*PSI*$^{+}$].

Keywords: Amyloid, Gγ, heat shock, Lsb2, mnemon, prion, RAC, Ssb, Ure2, yeast.

1. Introduction

Mammalian prions are transmissible infectious protein isoforms that cause transmissible spongiform encephalopathies (TSEs) and are based on self-perpetuating cross-β fibrous aggregates (amyloids) [1]. Amyloids associated with devastating human disorders such as Alzheimer's or Parkinson's diseases also possess certain prion features [2, 3]. Yeast *Saccharomyces cerevisiae* contains a variety of endogenous prions, that are heritable in a non-Mendelian fashion and frequently control detectable phenotypic traits [4, 5]. Therefore, yeast prions represent a protein-based pathway of inheritance, that is based on templated structures rather than on sequences. Majority of known yeast prions are amyloids, thus providing an excellent model for studying the biological and pathological aspects of amyloid formation [6]. Some prions are lethal or highly pathogenic in yeast [7, 8], while other prions have been proposed to play adaptive roles [9]. [*PSI*$^{+}$] and [*URE3*] are the best characterized yeast prions, based on amyloid forms of the translation termination factor Sup35 (eRF3), and regulatory protein in nitrogen uptake, Ure2, respectively [4, 5]. The stress-inducible short-living actin-associated yeast protein Lsb2 can also form a metastable prion, [*LSB*$^{+}$], that is inducible by heat treatment and is maintained in a fraction of the cell population recovered from heat shock, thus generating the cellular memory of stress [10].

In addition to prions, yeast cells contain non-heritable protein aggregates termed mnemons. While molecular foundations of prions and mnemons are similar to each other, mnemons stay in a mother cell and are not transmitted to daughters during a cell division [11]. Mnemon formed by Whi3 protein is responsible for the memory of failed mating [12]. We have previously demonstrated that a detergent-resistant aggregate of Ste18, the γ subunit of the heterotrimeric G-protein complex, also involved in the mating pathway, could be induced by protein overproduction and behaves as a non-heritable mnemon [13].

Heritability of yeast prions (in contrast to mnemons) is dependent on their interaction with the chaperone machinery. The concerted action of the cytosolic chaperones Hsp104, Hsp70-Ssa and Hsp40 (Sis1 or Ydj1) results in fragmentation of amyloid fibrils into oligomers, initiating new rounds of fibril growth [14]. This process is responsible for the propagation of most yeast amyloid-based prions and their transmission in cell divisions. At least in case of Sup35 prion, [*PSI*$^{+}$] Sis1 and Ssa bind to fibrils first and then recruit Hsp104, that pulls out Sup35 molecules thus promoting fibril fragmentation [15, 16]. Therefore, balance between these chaperones is crucial for the prion propagation and transmission. Both inactivation and overproduction of Hsp104 lead to the loss of [*PSI*$^{+}$]; Hsp104 inactivation also eliminates most other yeast amyloid-based prions, although some of them are not sensitive to the Hsp104 overproduction [14, 17].

In addition to Ssa, yeast cells contain another cytosolic member of the Hsp70 family, Ssb, that is ribosome-associated and directly participates in co-translational folding of nascent polypeptide chains [18]. This function of Ssb requires an interaction with the ribosome associated chaperone complex (RAC), composed of Hsp40-Zuo1 and noncanonical Hsp70, Ssz1 [19, 20]. The Ssb-RAC complex is also associated with the recruitment of ubiquitin ligase Ltn1, the major component of ribosome associated protein quality control (PQC) that detects aberrations in nascent chains and leads to their ubiquitination and degradation [21]. Ssb is encoded by two nearly identical genes, *SSB1* and *SSB2* [22]. We have previously demonstrated that both spontaneous and overproduction-induced formation of the Sup35 prion, [*PSI*$^{+}$] is increased in the cells having both Ssb-coding genes deleted, *ssb1/2Δ* [23]. Accordingly, Ssb overproduction enhanced [*PSI*$^{+}$] elimination in the presence of excess Hsp104 [23] and antagonized some variants of [*PSI*$^{+}$] on its own [24, 25]. Deletion of either *SSZ1* or *ZUO1* (or both) promoted formation of [*PSI*$^{+}$], similar to *ssb1/2Δ* [26, 27], however antagonized propagation of at least some [*PSI*$^{+}$] variants [27]. Notably, the latter effect depended on the presence of Ssb, suggesting that it occurs due to relocation of Ssb from the ribosome to cytosol in the RAC-deficient strains. We have demonstrated that

cytosolic Ssb interferes with binding of Ssa to the Sup35 prion aggregates, that may explain its antagonistic effect on [*PSI*$^{+}$] propagation [27, 28]. Partial relocation of Ssb from the ribosomes to cytosol was also detected in some unfavorable conditions, including heat shock, and coincided with destabilization of some [*PSI*$^{+}$] variants [27, 29]. Notably, heat-shock induced destabilization of [*PSI*$^{+}$] was greatly increased in the strains with RAC alterations (*zuo1Δ* and/or *ssz1Δ*) but decreased in the *ssb1/2Δ* cells, implicating Ssb relocation as a major factor modulating prion maintenance during stress [29]. Recent work by Wickner lab [30] demonstrated that majority of [*PSI*$^{+}$] isolates obtained in the *ssb1/2Δ* or *zuo1Δ* strains are destabilized by reintroduction of Ssb or Zuo1, respectively. These data consistently point to the role Ssb and RAC as an anti-prion system, antagonizing formation and propagation of the [*PSI*$^{+}$] prion. However, the deletion of the gene coding for the RAC component Ssz1 did not impact the formation of [*URE3*] prion [30], leading to the suggestion that the anti-prion effects of Ssb and RAC could be restricted to the proteins intimately associated with the translational machinery, such as Sup35.

Here, we present the results of systematic analysis of the effects of Ssb on the formation and propagation of self-perpetuating aggregates by proteins that are not associated with the translational machinery, namely Lsb2, Ste18 and Ure2. Our data show that Ssb is a major modulator of the formation and propagation of a variety of self-perpetuating protein aggregates in yeast.

2. Results

2.1 Effects of Ssb on the Lsb2 aggregation and prion formation.

Since Ssb is known to counteract the formation and propagation of the [*PSI*$^{+}$] prion, we checked if it influences self-perpetuating aggregates formed by other proteins. Lsb2 is a cytoskeleton-associated protein, that forms a metastable prion, [*LSB*$^{+}$] after transient overproduction or in response to heat stress [10, 31]. While the [*LSB*$^{+}$] prion has no obvious

phenotypic manifestation, it can be detected by its ability to promote [*PSI*$^{+}$] formation in the presence of excess Sup35 or Sup35N in [*pin*$^{-}$] cells lacking any other pre-existing prions such as [*PIN*$^{+}$], a prion form of Rnq1 protein [32, 33]. Aggregation of Lsb2 can also be detected biochemically and, in the case of the fluorophore-tagged Lsb2 derivative, cytologically. Lsb2 is a short-lived heat- inducible protein. We have demonstrated that levels of Lsb2 are increased in the

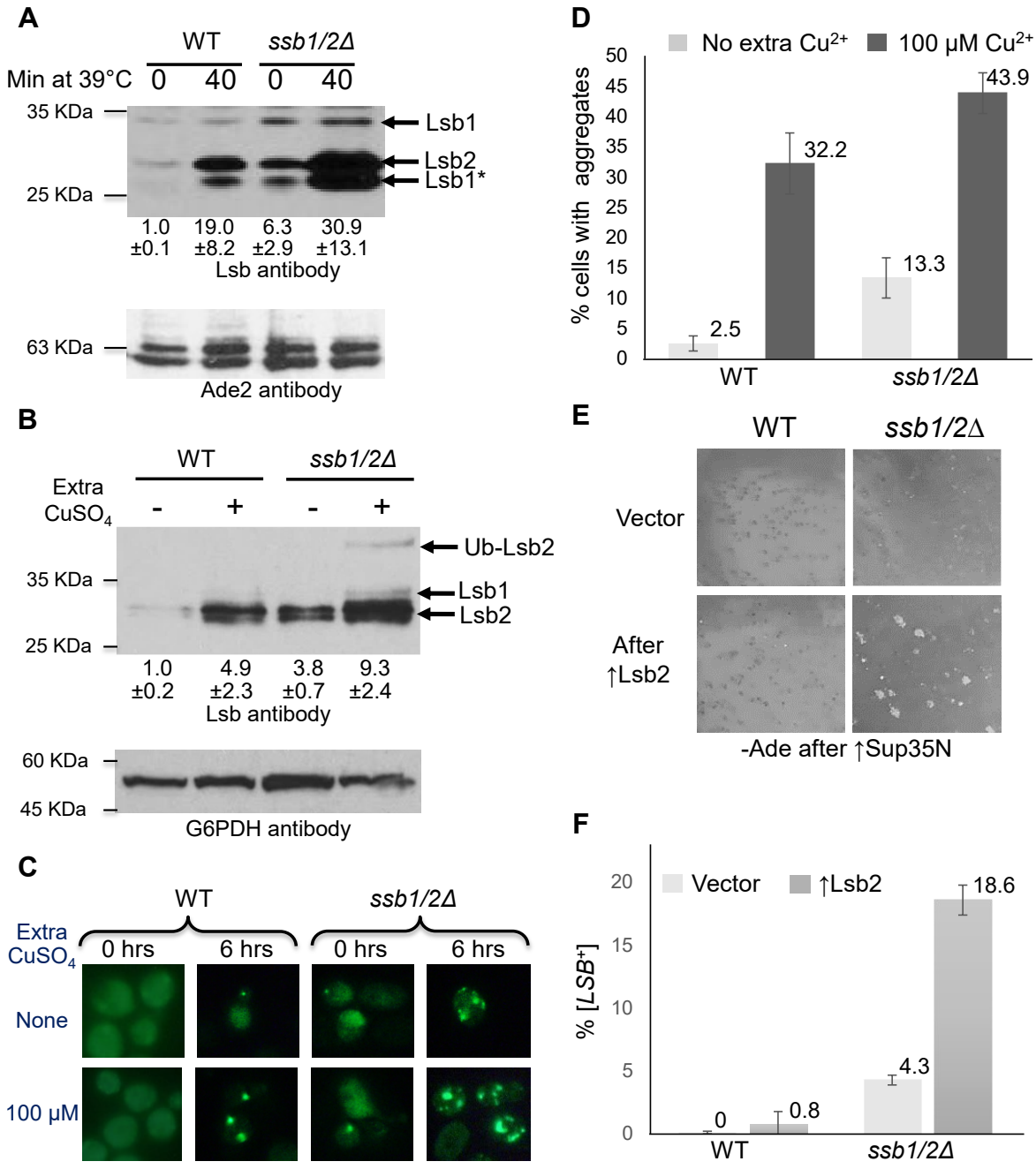

Figure 1. Effects of the *ssb1/2Δ* deletion on Lsb2 protein levels, aggregation, and prion induction. (A) and (B) Comparison of the levels of Lsb2 protein in WT and *ssb1/2Δ* strains before and after 40-min heat shock at 39°C (A), and with (in the presence of 150 μM $CuSO_4$) or without overexpression of *LSB2* from the Cu^{2+}-inducible promoter, P_{CUP1} (B). Proteins were detected by SDS-PAGE and Western blotting, followed by reaction to Lsb-specific antibodies, which recognizes Lsb2, ubiquitinated Lsb2 (Ub-Lsb2, as seen in the *ssb1/2Δ* sample upon overproduction on panel B), and full-length or processed (Lsb1*) isoforms of Lsb1 as indicated. On panel B, Lsb1* isoform is not separable from Lsb2 but should constitute a minor fraction in the absence of heat shock. The Ade2 (A) or G6PDH (B) proteins were used as loading controls. The second band seen on the Ade2 image represents a proteolytic product, detected in most experiments. Numbers under the gel indicate the results of normalized densitometry measurements shown as a ratio to the normalized Lsb2 levels in the WT strain without heat shock (a mean of at least three repeats with a standard deviation is shown in each case). Positions of the molecular weight markers are indicated on the left of each gel. (C) and (D) Formation of cytologically detectable aggregates of GFP-tagged Lsb2, expressed from the Cu^{2+} inducible P_{CUP1} promoter is increased in the *ssb1/2Δ* cells. On panel D, means and standard deviation are shown for three cultures in each strain/plasmid combination, after incubation in the liquid -Ura medium with or without extra Cu^{2+} added (as indicated), for 24 hours at 30°C. See Table S1 for numbers. (E) and (F) Induction of [*LSB*$^+$] prions after transient production of HA-Lsb2 from the P_{CUP1} promoter plasmid with or without addition of 150 μM $CuSO_4$ in WT and *ssb1/2Δ* strains. Means and standard deviation are shown for at least four cultures in each strain/plasmid combination. See Table S2 for numbers.

cells lacking Ssb, both at normal and increased temperature, when chromosomal *LSB2* is expressed from its endogenous promoter (Fig. 1A), and in the absence or in the presence of additional Cu^{2+} when plasmid-borne *LSB2* is expressed from a copper-inducible P_{CUP1} promoter (Fig. 1B). Additionally, microscopic observation showed that a proportion of cells with cytologically detectable aggregates of GFP-tagged Lsb2 was increased in the *ssb1/2Δ* strain compared to the isogenic WT strain, both at low and increased levels of Cu^{2+} (Fig. 1, C and D, and Table S1).

Next, we employed an assay for [*PSI*$^+$] cross-seeding in order to compare frequencies of the induction of [*LSB*$^+$] prions by transient overproduction of Lsb2 from the P_{CUP1} promoter in the wild-type (WT) and *ssb1/2Δ* strains. Both strains were lacking any detectable pre-existing prions ([*psi*$^-$ *pin*$^-$]) and contained the plasmid with the DNA fragment coding for the prion domain of Sup35 protein (Sup35N) placed under the control of galactose-inducible (P_{GAL}) promoter. Lsb2 overproduction was induced by growth in the presence of increased concentrations of $CuSO_4$ in glucose medium, where the P_{GAL}-*SUP35N* was silent. After overproduction, cells were plated onto the solid glucose medium with low concentration of $CuSO_4$ (where both P_{CUP1}-*LSB2* and

P_{GAL}-*SUP35N* are turned off). Grown colonies were transferred to the galactose medium where P_{GAL}-*SUP35N* construct is induced, followed by velveteen replica plating to the glucose medium lacking adenine (–Ade) medium for [*PSI*$^+$] detection. Sup35N overproduction efficiently induces formation of [*PSI*$^+$] prion only in the presence of another aggregated protein (in this case, Lsb2).

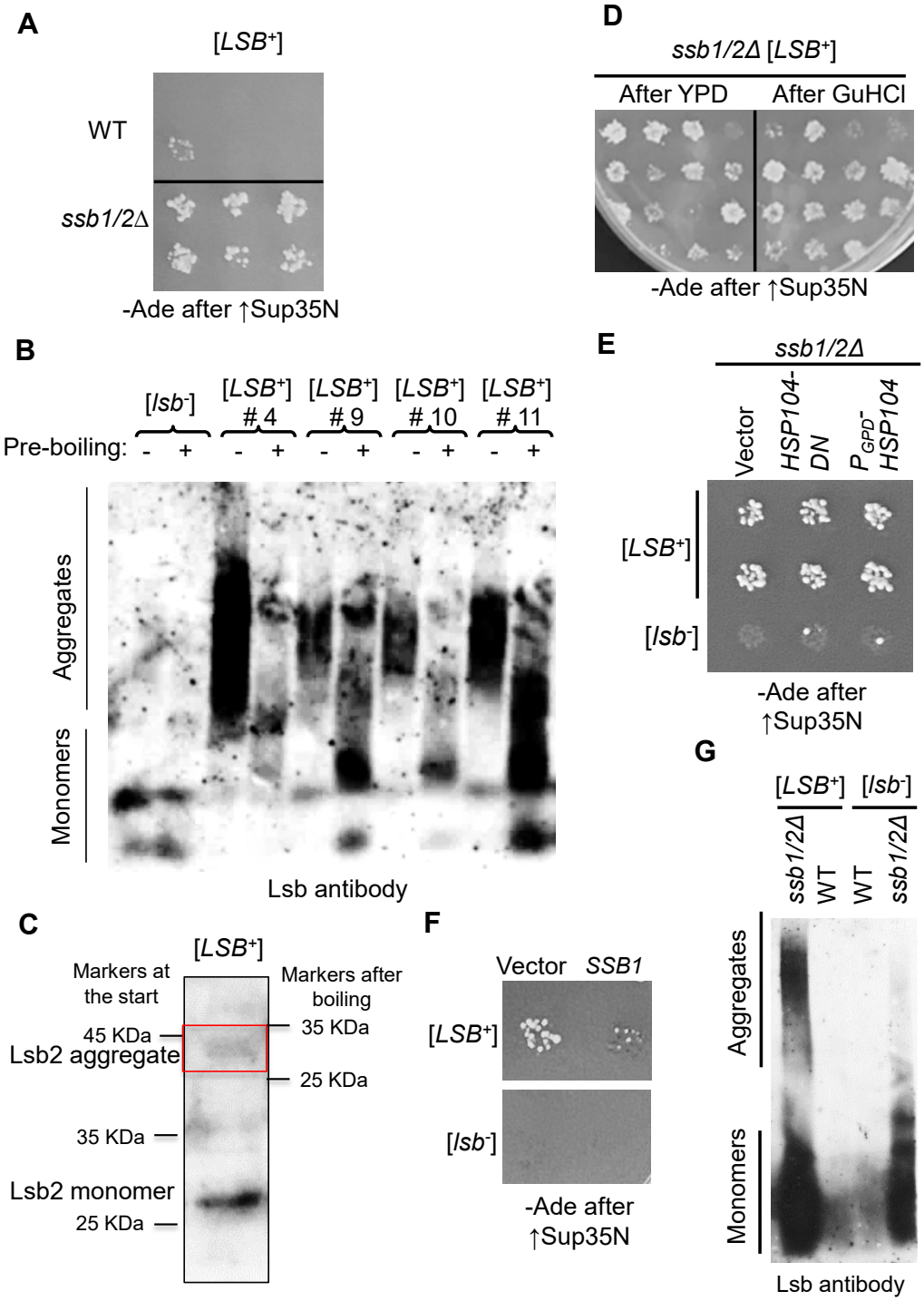

Figure 2. Mitotic stability and aggregate accumulation by the [*LSB*$^+$] prion in the presence and in the absence of Ssb. (A) Comparison of mitotic stabilities of the [*LSB*$^+$] prions obtained in WT and *ssb1/2Δ* strains, showing that most subcolonies obtained from the *ssb1/2* [*LSB*$^+$] (but not from the WT [*LSB*$^+$]) isolate retain their ability to promote [*PSI*$^+$] formation, indicating the presence of the [*LSB*$^+$] prion. For numbers, see Table S3. (B) Detection of the Lsb2 protein aggregates in the [*LSB*$^+$] strains and their solubilization by boiling. Proteins were isolated from the *ssb1/2Δ* [*LSB*$^+$] and original [*lsb*$^-$] strain, bearing the P_{CUP1}-*HA-LSB2* plasmid but grown without extra $CuSO_4$, and heat shocked for 40 min at 39°C in order to maximize the Lsb2 levels without overexpressing plasmid-borne *LSB2*. Pre-boiled (+) or not pre-boiled (-) samples were fractionated on the SDD-AGE gel, followed by a reaction to the Lsb antibody. (C) Detection of the Lsb2 protein aggregates in the [*LSB*$^+$] isolate after the loss of P_{CUP1}-*HA-LSB2* plasmid by the 'boiled gel" assay (see Materials and Methods). Positions of molecular weight markers loaded at the start of electrophoresis (left) or after boiling the gel (right) are shown; Lsb2 monomers and aggregates are indicated. (D) Retention of the [*LSB*$^+$] prion in subcolonies obtained by streaking on –Trp medium (selective for the resident *TRP1* P_{GAL}-*SUP35N* plasmid) after three passages on either YPD medium or YPD with 2 mM GuHCl, as indicated. Presence of [*LSB*$^+$] in the subcolonies was checked by the [*PSI*$^+$]-induction assay (see Materials and Methods). The representative example is shown. See Table S4 for numbers. (E) Transient inactivation of Hsp104 by dominant negative *HSP104-DN* allele, or overexpression of wild-type Hsp104 (both produced from the highly expressed P_{GPD}) promoter does not affect the [*LSB*$^+$] prion in the *ssb1/2Δ* background. The experiment was performed by mating assay as described in Materials and Methods. Five [*LSB*$^+$] subcolonies from each of two independent [*LSB*$^+$] isolates were tested, with similar results. A representative image with two [*LSB*$^+$] subcolonies and [*lsb*$^-$] control is shown. (F) Reintroduction of Ssb1 antagonizes the [*LSB*$^+$] prion, obtained in the *ssb1/2Δ* background. The experiment was performed by mating assay as described in Materials and Methods. Five independent [*LSB*$^+$] isolates were tested, and 4 of them exhibited an inhibitory effect of Ssb on [*LSB*$^+$]. A representative example is shown. (G) Reintroduction of Ssb abolishes the detergent-resistant Lsb2 aggregates. The [*LSB*$^+$] and [*lsb*$^-$] isolates of the *ssb1/2Δ* strain were mated with the isogenic [*psi*$^-$ *pin*$^-$] WT and *ssb1/2Δ* strains of the opposite mating type, and grown in the absence of extra $CuSO_4$, followed by protein isolation, fractionation on the SDD-AGE gel and reaction to the anti-Lsb antibody.

[*PSI*$^+$] cells could be detected by their ability to grow on –Ade medium, due to impaired termination function of the Sup35 protein in prion form, resulting in readthrough of the *ade1-14* (UGA) reporter construct [4]. Thus, growth on –Ade following the Sup35N overproduction indicated the presence of the Lsb2 prion, [*LSB*$^+$] in the cells of a respective colony. Notably, formation of the phenotypically detectable [*LSB*$^+$] prions after transient overproduction of Lsb2 was significantly increased in the *ssb1/2Δ* background, compared to the isogenic WT strain (Fig. 1, E and F, and Table S2). The [*LSB*$^+$] isolates obtained in the WT strain were highly unstable and essentially completely lost the [*LSB*$^+$] prion after colony purifying (Fig. 2A and Table S3), as described previously [10]. In contrast, the [*LSB*$^+$] isolates obtained in the *ssb1/2Δ* strain exhibited high mitotic stability (Fig. 2A and Table S3), with most colonies retaining the [*LSB*$^+$] prion even

after loss of the P_{CUP1}-*LSB2* plasmid. Notably, all 5 tested [*LSB*$^+$] isolates obtained in the *ssb1/2Δ* background contained detergent-resistant Lsb2 aggregates (see examples on Fig. 2B), detectable by semi-denaturing detergent agarose gel electrophoresis, SDD-AGE [34], and 4 of them retained detectable aggregates after the loss of the P_{CUP1}-*LSB2* plasmid as shown by both SDD-AGE and "boiled gel" SDS-PAGE (see an example on Fig. 2C). Lsb2-reactive material was shifted to the lower molecular weight fraction after pre-boiling the sample before loading onto the SDD-AGE gel (Fig. 2B). This indicates that Lsb2 aggregates were at least partially solubilized by pre-boiling, confirming their non-covalent nature. Surprisingly, the [*LSB*$^+$] isolates generated in the *ssb1/2Δ* background were not curable by growth in the presence of the anti-prion agent, GuHCl (Fig. 2D and Table S4). In contrast, the [*PSI*$^+$] prions formed in the *ssb1/2Δ* [*LSB*$^+$] strain were curable by GuHCl as expected (Fig. S1 and Table S5). GuHCl is an inhibitor of the chaperone Hsp104 [35, 36], playing a crucial role in the propagation of [*PSI*$^+$] and most other amyloid-based yeast prions known to date [4, 14]. We have also tested the effect of Hsp104 on the [*LSB*$^+$] prions, obtained in the *ssb1/2Δ* background. Neither expression of the dominant negative allele of *HSP104* (*HSP104-DN*), nor constitutive overexpression of *HSP104* from the P_{GPD} promoter efficiently cured [*LSB*$^+$] in the *ssb1/2Δ* strain (Fig. 2E). This was in contrast to the Rnq1 prion, [*PIN*$^+$] that was efficiently cured by *HSP104-DN* in the same experimental design (Fig. S2). Thus, at least in the *ssb1/2Δ* background, the [*LSB*$^+$] prions are completely or partially independent of Hsp104. Notably, mating the *ssb1/2Δ* [*LSB*$^+$] strain either to isogenic Ssb$^+$ [*lsb*$^-$] strain of the opposite mating type, or to isogenic *ssb1/2Δ* [*lsb*$^-$] strain of the opposite mating type with the plasmid-bourne *SSB1* gene (Fig. 2F) led to the significant decrease of [*PSI*$^+$]-inducing activity, indicating the high frequency of loss of the [*LSB*$^+$] prion. Likewise, Lsb2 aggregates detectable by SDD-AGE disappeared after mating the *ssb1/2* [*LSB*$^+$] strain to the WT (Ssb$^+$) stain of the opposite mating type, but not after mating to the isogenic *ssb1/2Δ* strain (Fig. 2G). These results show that Ssb antagonizes the propagation of [*LSB*$^+$] prions generated in the absence of Ssb.

2.2 *Effects of Ssb on the altered derivatives of Lsb2.*

Next, we checked if mutational alterations of Lsb2 impact the effect of Ssb on prion formation. For this purpose, we employed a series of the mutant derivatives of HA-tagged Lsb2 protein, expressed from the P_{CUP1} promoter in WT and *ssb1/2Δ* cells, either in the presence or in the absence of the endogenous chromosomal copy of *LSB2*. Examples shown on Fig. 3, A and B, and densitometry analysis of data indicated that levels of HA-Lsb2 induced by $CuSO_4$ were increased at 3.3-fold in the example shown on Fig. 1A, and at 1.8-fold on average in the *ssb1/2Δ* background, compared to the Ssb^+ cells. This increase was statistically significant ($p<0.01$

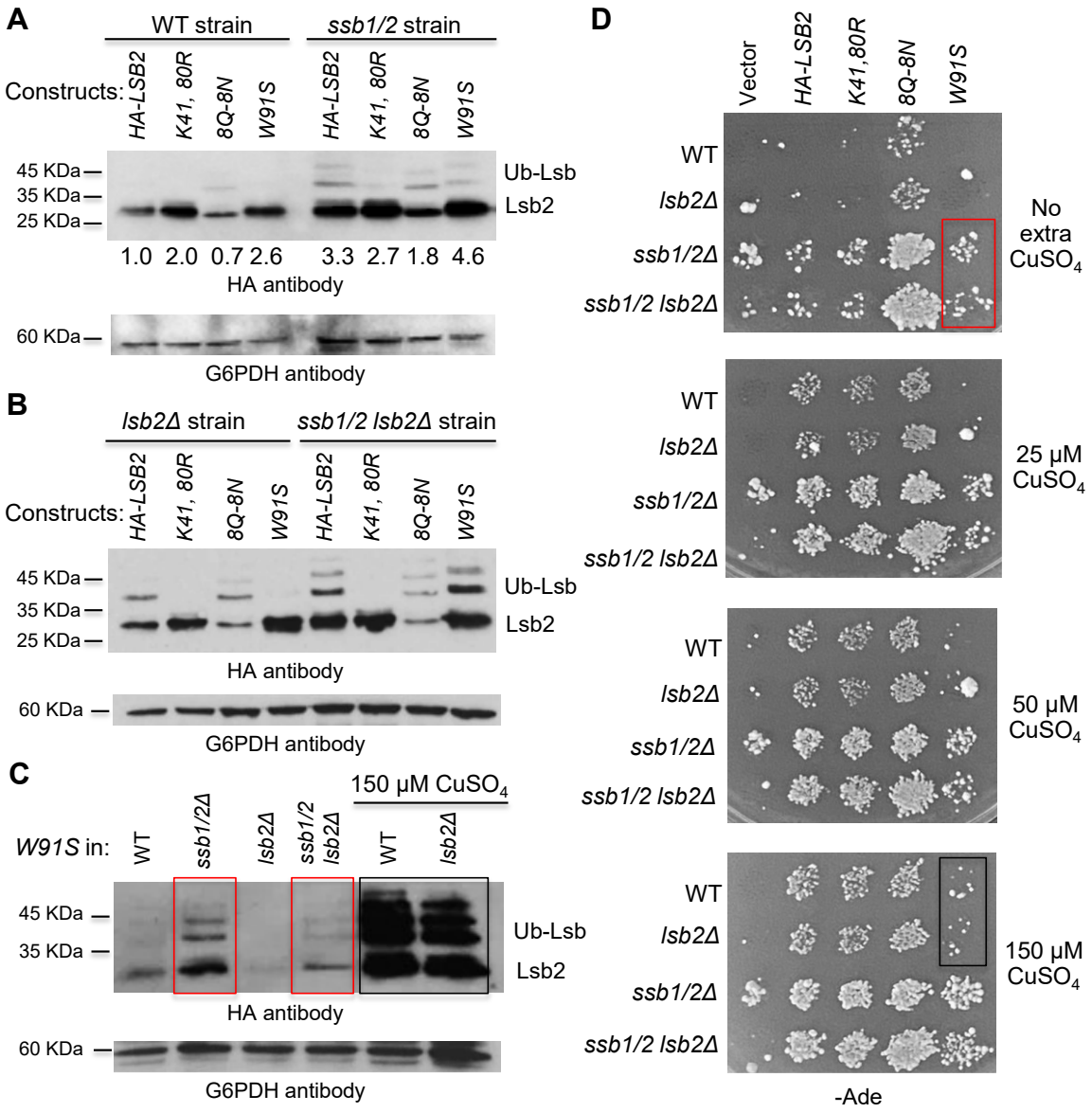

Figure 3. Effects of mutations on the Lsb2 protein levels and prion formation in the presence and in the absence of the Ssb protein. (A) and (B) Levels of HA-reactive material in the Lsb$^+$ (A) and *lsb2Δ* (B) strains expressing the wild type *LSB2* gene or its mutant (*K41,80R, 8Q-8N*, and *W91S*) derivatives (as indicated) from the P_{CUP1} promoter on a plasmid, when grown with the addition of 150 μM $CuSO_4$. Proteins were detected by SDS-PAGE and Western blotting, followed by reaction to HA antibody. Positions of the molecular weight markers and of ubiquitinated Lsb2 (Ub-Lsb2) are indicated. Densitometry values calculated for normalized HA-Lsb2 and its derivatives relative to normalized wild-type HA-Lsb2 levels in the WT strain are provided for the gel shown on panel A as an example. (C) Comparison of the levels of WT and W91S mutant HA-Lsb2 derivatives expressed from the P_{CUP1} promoter at low and high (after addition of 150 μM $CuSO_4$) levels of Cu^{2+} both in the presence and in the absence of chromosomal *LSB2* and/or *SSB1/2*. On panels A-C, the levels of G6PDH protein in the same samples are shown as a loading control. (D) Effects of the Lsb2 mutations on the [*LSB*$^+$] induction as detected in the sequential overproduction protocol (see Fig. S3). Respective constructs were expressed from the P_{CUP1} promoter in the presence of indicated amounts of $CuSO_4$ in the WT and *ssb1/2Δ* strains, either containing or lacking chromosomal *LSB2* (as shown) and bearing the P_{GAL}-*SUP35N* plasmid. This was followed by turning the P_{CUP1}-mediated overexpression off and turning the P_{GAL}-*SUP35N* overexpression on after velveteen replica plating yeast cultures to the galactose medium lacking extra $CuSO_4$. Then, plates were velveteen replica plated to -Ade allowing detection of [*LSB*$^+$] by its ability to induce [*PSI*$^+$]. Squared are protein levels (C) and [*PSI*$^+$] induction results (D) for cultures expressing HA-Lsb2-W91S at high levels in the Ssb$^+$ background (black squares) and cultures expressing HA-Lsb2-W91S at low levels in the *ssb1/2Δ* background (red squares).

according to sign-test [37]) as it has been observed in all 8 repeats of the experiment. This confirms that levels of *LSB2* are elevated in the absence of Ssb even when it is expressed exclusively from a heterologous promoter. The following mutants were tested in our work: a) double substitution K41R K80R (designated here and further as K41,80R), knocking out major ubiquitination sites of Lsb2; b) the 8Q-8N derivative, having the stretch of eight Q residues at positions 172-179 substituted by a stretch of eight N residues, and known to increase mitotic stability of [*LSB*$^+$] prions [10, 31]; and c) the W91S substitution, disrupting an interaction of Lsb2 with actin cytoskeleton through Las17 protein, and shown by us to knock out Lsb2 aggregation and its ability to cross-seed [*PSI*$^+$] [31].

In line with previous observations [31], the K41,80R derivative of HA-Lsb2 demonstrated an increase in protein levels (see examples on Fig. 3, A and B) in comparison to WT protein only in 5 out of 8 repeats, when induced by $CuSO_4$ from the P_{CUP1} promoter in the Ssb$^+$ strains. However, the ubiquitinated Lsb2 bands disappeared in the K41,80R mutant, confirming a defect in

ubiquitination (Fig. 3, A and B). The Cu^{2+}-induced W91S derivative of HA-Lsb2 derivative exhibited a statistically significant increase in protein levels (at 1.7-fold on average), compared to WT HA-Lsb2 in 8 out of 8 repeats (p<0.01) for the Ssb^+ strain (see examples on Fig. 3, A and B). Neither K41,80R nor W91S derivative did show a systematic difference in levels from the WT protein at high levels of induction in the absence of Ssb. Notably, at background levels of $CuSO_4$, the W91S HA-Lsb2 derivative was accumulated at about 4-fold higher levels in the *ssb1/2Δ* cells, compared to Ssb^+ (Fig. 3C). Interestingly, the Cu-induced 8Q-8N HA-Lsb2 derivative was consistently expressed at lower level (about 0.6-fold on average) compared to the WT protein in both Ssb^+ and *ssb1/2*Δ strains (see examples on Fig. 3, A and B).

Next, we tested the impact of mutational alterations on the formation of Lsb2 prion in strains containing or lacking Ssb (Fig. 3D). For this purpose, we applied the sequential induction protocol [10]. This protocol employs the cultures containing both the *LSB2* constructs under the P_{CUP1} promoter, and the *SUP35N* construct under the P_{GAL} (galactose-inducible) promoter. The P_{CUP1} constructs are either expressed at low levels or induced at high levels on glucose medium containing low or increased concentrations of Cu^{2+}, respectively. This is followed by replica plating onto medium containing galactose with low concentration of Cu^{2+} (Fig. S3). Therefore, formation of [*PSI*$^+$], used as an indicator of the presence of [*LSB*$^+$], is detected in conditions when expression of Lsb2 is low, so that [*PSI*$^+$] could be induced only in the presence of a heritable [*LSB*$^+$] prion. This enables us to detect induction of heritable prions by transient overexpression of Lsb2. In line with previous observations [10, 31], our data (Fig. 3D) demonstrated that in the presence of Ssb, the K41,80R substitution did not significantly increase [*LSB*$^+$] formation in comparison to WT Lsb2, while 8Q-8N substitution led to a significant increase (even in the absence of extra $CuSO_4$), possibly due to increased mitotic stability of a prion. For both mutant derivatives, the [*LSB*$^+$] formation was increased further in the absence of Ssb (Fig. 3D). This suggests that the increase of [*LSB*$^+$] formation in the absence of Ssb is not solely due to increase in mitotic stability of [*LSB*$^+$],

because such increase is observed even for the 8Q-8N derivative that is normally producing prions with high mitotic stability.

In agreement with our previous data [31], the W91S derivative of HA-Lsb2 promoted [*LSB*$^+$] formation neither in the presence nor in the absence of WT Lsb2 in the Ssb$^+$ strain (Fig. 3D). However, the W91S derivative of HA-Lsb2 was able to promote the formation of [*LSB*$^+$] prion in the *ssb1/2Δ* background, more efficiently in the case when endogenous Lsb2 was present (Fig. 3D). Moreover, HA-Lsb2-W91S induced the formation of [*LSB*$^+$] in the *ssb1/2Δ* strains even at low concentration of Cu^{2+} (Fig. 3D), despite that the levels of HA-Lsb2-W91S protein in these cells were significantly lower than in the Ssb$^+$ cells grown at high concentrations of Cu^{2+} (Fig. 3C) where promotion of the [*LSB*$^+$] formation by this protein was not detected (Fig. 3D). These results confirm that the absence of Ssb indeed enhances prion-forming propensities of Lsb2-derived constructs, rather than simply operating via an increase in protein levels.

2.3 Prion induction by heat stress in the ssb1/2Δ background.

Our previous data indicated that the formation of [*LSB*$^+$] prion is induced by heat stress [31], while *ssb1/2Δ* increases mitotic stability of the [*PSI*$^+$] prion after heat shock [29]. Therefore, we checked if the generation of prions capable to cross-seed *de novo* formation of [*PSI*$^+$] (as described for [*LSB*$^+$]) after heat stress is increased in the absence of Ssb. For this purpose, the cultures of WT, *ssb1/2Δ* and *ssb1/2Δ lsb2Δ* strains lacking known prions ([*pin*$^-$]) and bearing the *TRP1* P_{GAL}*-SUP35N* construct were grown in complete YPD medium and incubated for 2 hrs at 39^{o}C. Samples of both heat-stressed culture and a culture before treatment were then plated onto glucose –Trp medium at 30^{o}C, followed by the induction of P_{GAL}*-SUP35N* on galactose medium, -Trp+Gal (see Materials and Methods). As overexpression of Sup35N promotes formation of [*PSI*$^+$] only in the presence of another prion, growth on –Ade medium after galactose induction was indicative of the generation of a prion (capable to cross-seed [*PSI*$^+$] and designated [*PRN*$^+$]) in the progenitor cell for a given colony. Our data confirmed that heat stress increases formation

of [*PRN*$^+$] prions and showed that both spontaneous and heat-induced formation of [*PRN*$^+$] is significantly increased in the *ssb1/2Δ* culture, compared to WT culture (Fig. 4A and B). Notably, only a slight (and in case of heat stress, statistically insignificant) increase in [*PRN*$^+$] formation was detected in the *ssb1/2Δ lsb2Δ* strain, compared to the WT strain (Fig. 4A and Table S6). These results indicate that *ssb1/2Δ* greatly promotes formation of new prions in yeast cells in an Lsb2-dependent manner. Increased formation of [*PRN*$^+$] was especially pronounced after heat stress, when up to 17% of the *ssb1/2Δ* cells contain such a prion. About two-thirds of [*PRN*$^+$]

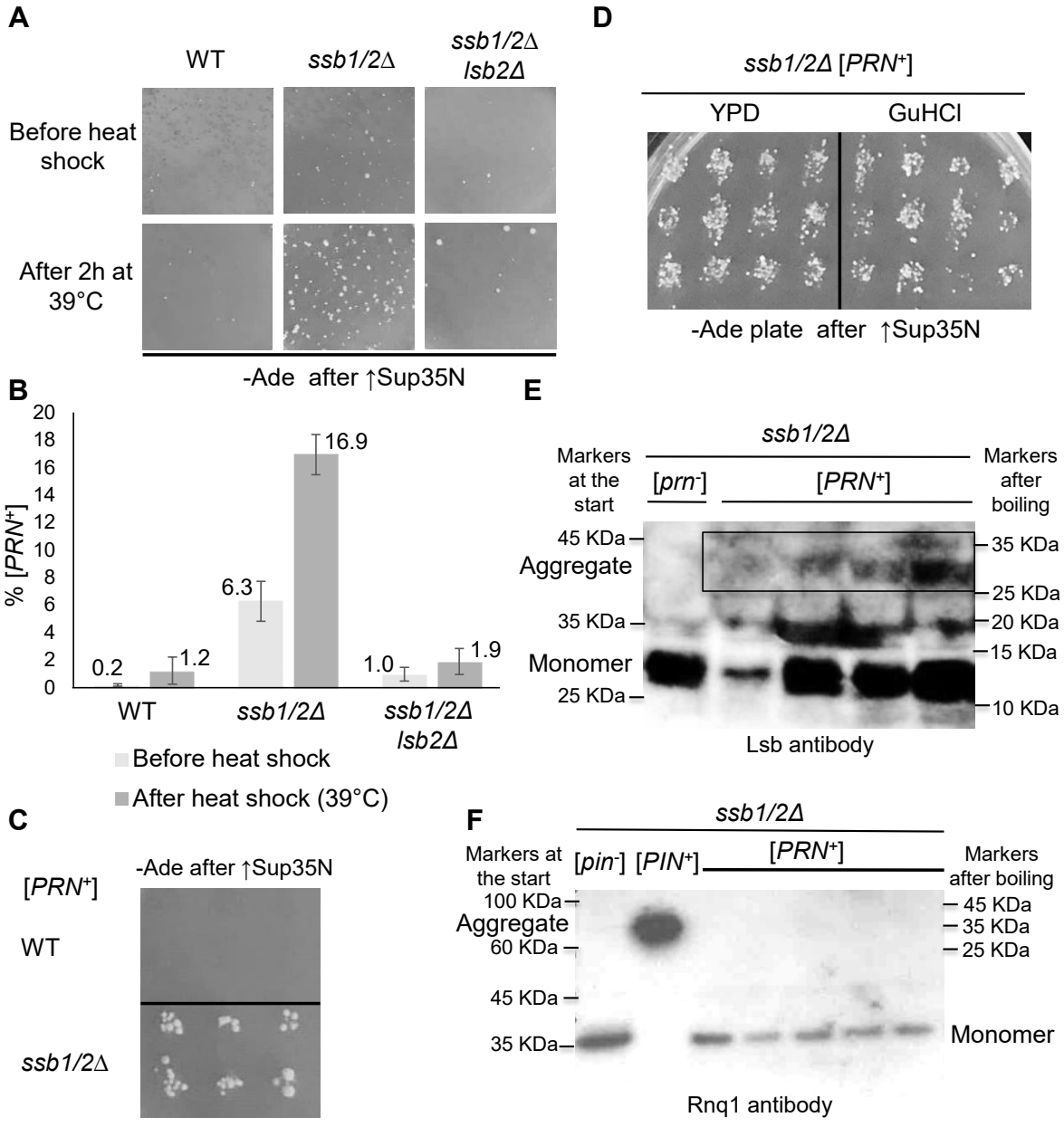

Figure 4. Effect of *ssb1/2Δ* on prion formation during heat shock. (A and B) Induction of derivatives with [*PSI*$^+$]-inducing capacity ([*PRN*$^+$]) during heat shock in the WT and *ssb1/2Δ* strains, either containing or lacking *LSB2*. Colonies obtained from heat-treated (2 hrs at 39°C) and control cells are shown on -Ade medium after overexpression of P_{GAL}-*SUP35N* construct are shown on panel (A), while frequencies of [*PRN*$^+$] colonies are shown on panel (B; error bars indicate standard deviation. Frequency of [*PRN*$^+$] is increased in the *ssb1/2Δ* background, and most [*PRN*$^+$] prions depend on *LSB2*. For numbers, see Table S6. (C) Mitotic stability of the [*PRN*$^+$] isolates are increased in *ssb1/2Δ* strain. Subcolonies of one typical WT [*PRN*$^+$] isolates and one typical *ssb1/2Δ* [*PRN*$^+$] isolate are shown as an example. For numbers, see Table S3. (D) [*PRN*$^+$] prion is not curable by GuHCl in the *ssb1/2Δ* background. Procedure is the same as on Fig. 2D. Subcolonies of one typical *ssb1/2Δ* [*PRN*$^+$] isolate are shown as an example. For numbers, see Table S4. (E and F) Most [*PRN*$^+$] prions contain aggregates of Lsb2, but not of Rnq1. Examples of the "boiled gel" analysis of the *ssb1/2Δ* [*PRN*$^+$] isolates is shown with Lsb (E) and Rnq1 (F). Positions of molecular weight markers loaded at the start of electrophoresis are shown on the left; positions of molecular weight markers loaded after boiling the gel are shown on the right. Positions of Lsb2 (visible aggregates are boxed) and Rnq1 monomers and aggregates are indicated.

isolates obtained in the *ssb1/2Δ* background were characterized by moderate (12– 29%) mitotic stability (Fig. 4C and Table S3), while rare [*PRN*$^+$] isolates obtained in the WT strain were completely unstable and lost the [*PRN*$^+$] in essentially all of mitotic progeny. Similar to the [*LSB*$^+$] prions induced by transient overproduction of Lsb2, the mitotic loss of [*PRN*$^+$] isolates obtained in the *ssb1/2Δ* background was not increased in the presence of GuHCl (Fig. 4D and Table S4). In contrast, the [*PSI*$^+$] prions cross-seeded by these [*PRN*$^+$] isolates were curable by GuHCl in these same strains (Table S5). Seven (87%) out of eight *ssb1/2Δ* [*PRN*$^+$] isolates tested contained detergent-resistant Lsb2 aggregates that were detectable on either (or both) "boiled" SDS-PAGE gel ([38], see Materials and Methods) as shown on Fig. 4E, and/or on SDD-AGE gel (data not shown). This confirms that in a majority of the cases, a [*PRN*$^+$] prion generated during heat shock is in fact an [*LSB*$^+$] prion. It should be noted that the concentration of Lsb2 aggregates in the extracts of [*PRN*$^+$] cultures extracts was usually relatively low and comparable to the cells containing the proven [*LSB*$^+$] prion (induced by artificial overproduction of the Lsb2 protein) after the loss of the *LSB2* plasmid (see above, Fig. 2C). Therefore, it is possible that even [*PRN*$^+$] isolates not showing the Lsb2 aggregates simply contained these aggregates at even lower levels, escaping detection by SDD-AGE. In contrast to Lsb2, aggregates of Rnq1 (another yeast

protein, known to cross-seed [*PSI*$^{+}$] into a prion form, see [4]) were not detectable in the extracts of [*PRN*$^{+}$] isolates by the “boiled” SDS-PAGE gel assay (Fig. 4F). This confirms that the formation of [*PRN*$^{+}$] is typically not due to generation of a prion form of Rnq1.

2.4 Effects of Ssb on Ste18 aggregation.

Yeast Ste18 protein is a γ-subunit of G-protein, that is involved in the pheromone signaling pathway, and is shown by us [13] to form a non-heritable amyloid-like aggregate with properties of yeast mnemon upon overproduction. Similar to Lsb2, aggregated Ste18 can cross- seed Sup35 into a prion form, [*PSI*$^{+}$]. We have investigated the effect of *ssb1/2Δ* on Ste18 aggregation and on [*PSI*$^{+}$] cross-seeding by Ste18. Ste18, produced from the construct under the P_{CUP1} promoter, was essentially undetectable at low levels of Cu^{2+} in the WT strain, however it was induced by an increased concentration of Cu^{2+}. Notably, levels of Ste18 were increased in the *ssb1/2Δ* strain, both at low (so that it becomes detectable) and high (at about 1.5-fold) concentrations of Cu^{2+} (Fig. 5A). As described previously [22], Ste18 overproduction at high levels of Cu^{2+} resulted in accumulation of detergent-resistant aggregates, that could be visualized on an SDD-AGE gel and were more abundant in the *ssb1/2Δ* background (Fig. 5B). Aggregates of the GFP-tagged Ste18 construct could also be detected by fluorescence microscopy, and accumulation of cytologically detectable aggregates was increased in the *ssb1/2Δ* strain, compared to isogenic WT strain (Fig. 5C and D, and Table S7).

Two protocols have been employed for the detection of Ste18-dependent cross-seeding of [*PSI*$^{+}$] prion (Fig. S3), namely simultaneous overexpression, when both Ste18 and Sup35N were co-overexpressed in the same cell, and sequential overexpression, when Ste18 was overexpressed first, followed by induction of Sup35N after overexpression of Ste18 was turned off. The latter protocol was similar to one employed previously for Lsb2 and its mutant derivatives (Fig. S3 and Fig. 3C), and Lsb2 was used as a positive control in both protocols. In the WT strain, Lsb2 promoted [*PSI*$^{+}$] induction after both simultaneous and sequential overexpression, while

284 Ste18 cross-seeded [*PSI*$^{+}$] only in the simultaneous but not the sequential protocol (Fig. 6A). This

285 result agreed with our previous data [13] and was expected as aggregates of Ste18 are entirely

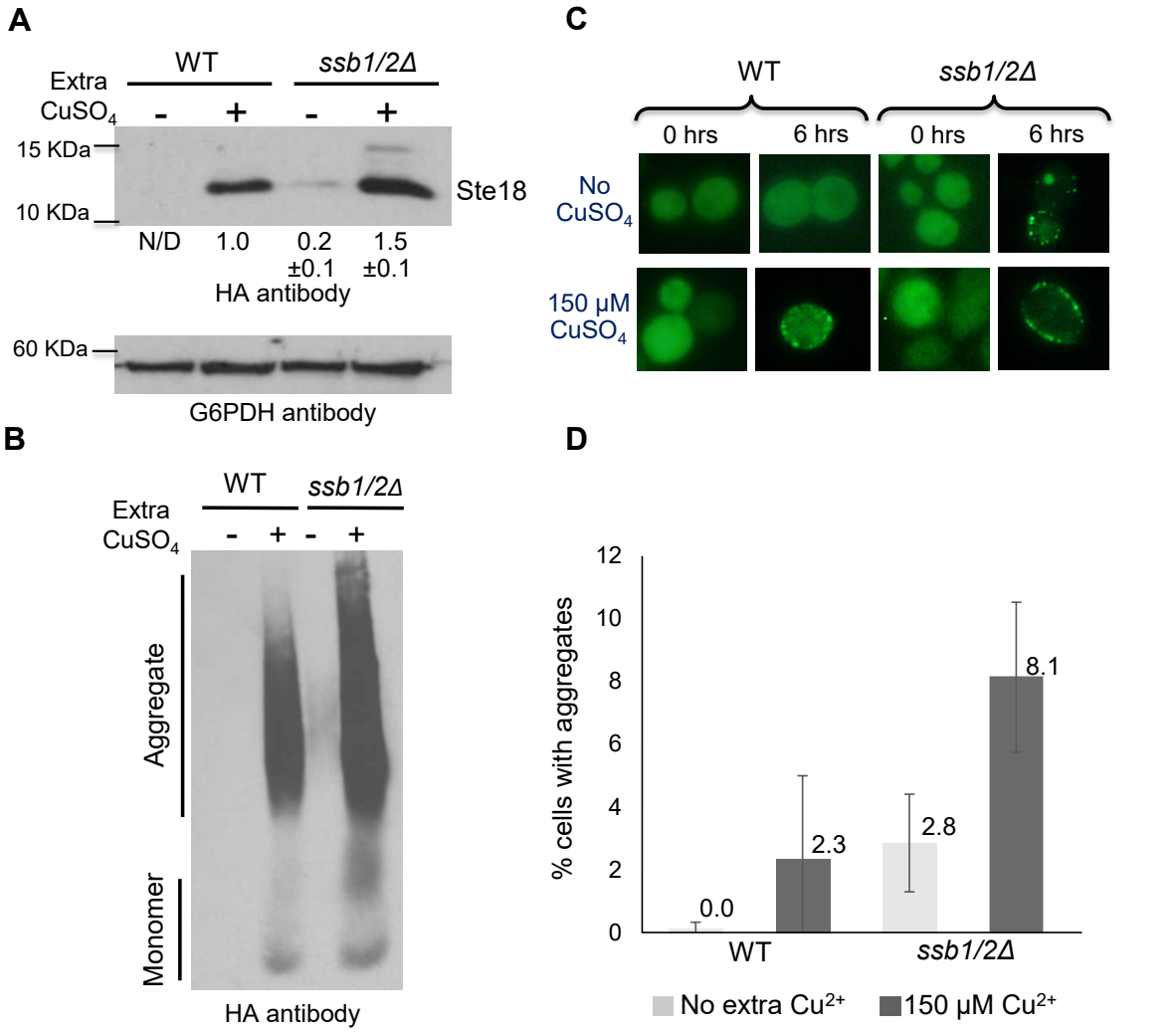

Figure 5. Effects of Ssb on levels and aggregation of the Ste18 protein. (A) Levels of HA-tagged Ste18 expressed from the construct under the P_{CUP1} promoter. Proteins were isolated from cultures grown in the plasmid-selective medium for 48 hrs without (-) or with (+) 150 μM $CuSO_4$ added, and analyzed by SDS-PAGE and Western blotting, followed by reaction to HA antibodies. Positions of molecular weight markers are indicated. Levels of G6PDH protein in the same samples are shown as a loading control. Ratios of Ste18 determined by densitometry and normalized by G6DPH are indicated, relative to the level of Ste18 in the WT strain with $CuSO_4$. Numbers correspond to a mean of three replicates with standard deviations. Ste18 was not detectable (N/D) in this experiment in the WT strain grown without addition of $CuSO_4$ (B) Detection of detergent-resistant aggregates of HA-Ste18 in the WT and *ssb1/2Δ* samples (obtained as shown on panel A) by SDD-AGE. (C and D) Detection of GFP-Ste18 aggregates by fluorescence microscopy. Cultures containing the plasmid with P_{CUP1}-*GFP-STE18* construct and grown with or without addition of 150 μM $CuSO_4$ for indicated periods of time are shown on panel C. Average frequencies (a mean of three independent replicates with a standard deviation) of cells with aggregates in cultures containing the P_{CUP1}-*GFP-STE18* plasmid and grown for 6 hrs either with or without addition of 150 μM $CuSO_4$ are shown on panel D. For numbers, see Table S7.

non-heritable in the WT strain, in contrast to aggregates of Lsb2 which are heritable. However, we found that overexpressed Ste18 is able to promote [*PSI*$^+$] formation both after simultaneous and after sequential overproduction in the *ssb1/2* background (Fig. 6A). This indicated that Ste18 aggregates formed after its overproduction have become heritable in the absence of Ssb.

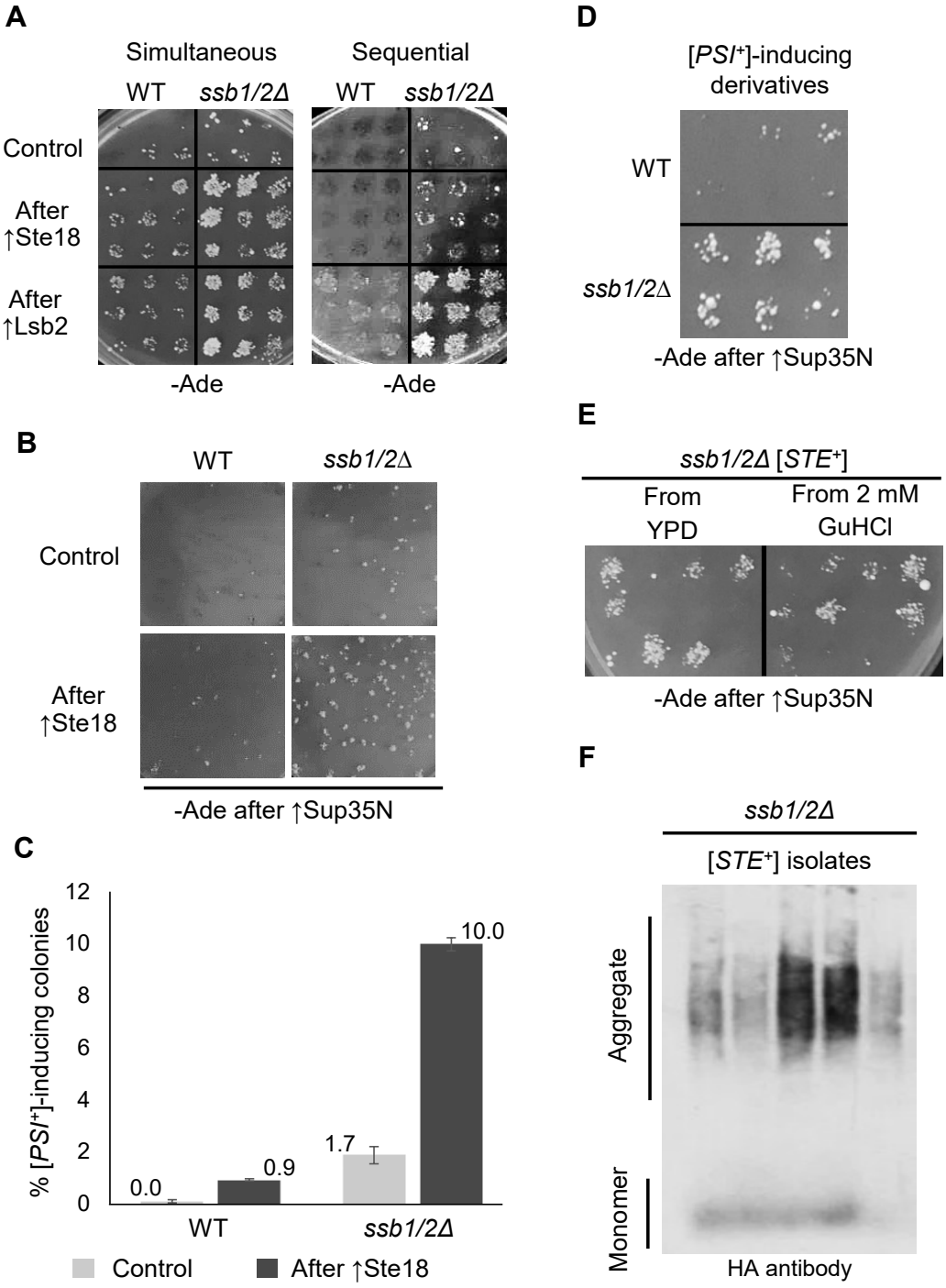

Figure 6. Effect of Ssb on the formation and heritability of the [*STE*$^+$] derivatives. (A) Formation of the [*STE*$^+$] derivatives (detected by the promotion of [*PSI*$^+$] induction) after transient overexpression of the P_{CUP1}-*HA-STE18* construct in accordance to either simultaneous (left) or sequential (right) induction protocol (see Fig. S3). In the simultaneous induction protocol, both Ste18 and Sup35N are overproduced together, while in the sequential induction protocol, Ste18 is overproduced first, followed by overproduction of Sup35N in the conditions when the Ste18 overproduction is turned off. Ste18 overproduction promotes [*PSI*$^+$] formation only in the simultaneous protocol in the WT strain, but in both simultaneous and sequential induction protocols in the *ssb1/2Δ* strain, indicating that Ste18 aggregates become partly heritable in the absence of Ssb. Empty vector is shown as a negative control, while vector overproducing Lsb2, which promotes [*PSI*$^+$] formation in both simultaneous and sequential induction assays in both WT and *ssb1/2Δ* strains, is shown as a positive reference. (B and C) Induction of [*STE*$^+$] colonies (detected by the ability to promote [*PSI*$^+$] formation) by transient overexpression of the P_{CUP}-*HA-STE18* construct after the addition of 150 μM $CuSO_4$ to the growth medium in the WT and *ssb1/2Δ* strains. Empty vector was used as a control. Cultures were grown for 24 hours in the presence of inducer. Percentages on panel C represent a mean of at least three independent cultures for each strain/plasmid combination, with bars showing standard deviation. For numbers, see Table S8. (D) The [*PSI*$^+$]-inducibility phenotype of colonies shown on panel B is mitotically heritable in the *ssb1/2Δ* (but not in the WT) background. Subcolonies of one typical colony, obtained on the medium selective for the plasmid (but without Cu^{2+} induction) are shown for each WT and *ssb1/2Δ* strains. Similar results were obtained without selection for the plasmid. For numbers, see Table S9. (E) [*STE*$^+$] prion is not curable by GuHCl in the *ssb1/2Δ* background. The experiment was performed in the same way as on Fig. 2D and Fig. 4D. A typical example is shown. For numbers, see Table S4. (F) The [*STE*$^+$] derivatives obtained as shown on panel B contain detergent-resistant aggregates of Ste18 protein. Proteins, isolated from [*STE*$^+$] derivatives of the *ssb1/2Δ* strain, containing the P_{CUP1}-*HA-STE18* plasmid and grown in the absence of extra $CuSO_4$ were run on the SDD-AGE gel with sodium N-lauroylsarcosine, followed by a transfer to the nitrocellulose membrane and a reaction to the HA antibody.

Indeed, up to 10% of colonies obtained after transient overproduction of Ste18 in the *ssb1/2Δ* strain were capable of [*PSI*$^+$] induction, compared to less than 1% of such colonies in the WT strain (Fig. 6, B and C, and Table S8). Moreover, most of [*PSI*$^+$]-inducing derivatives obtained in the WT background lost the ability to induce [*PSI*$^+$] after colony purification, while most [*PSI*$^+$]-inducing derivatives obtained in the *ssb1/2Δ* strain (and designated [*STE*$^+$]) were able to transmit the [*PSI*$^+$]-inducing ability to a majority of the mitotic progeny (Fig. 6D and Table S9). Notably, the *ssb1/2Δ* [*STE*$^+$] isolates exhibited high retention of the [*PSI*$^+$]-inducing phenotype even after the loss of the *STE18* plasmid, indicating that the [*STE*$^+$] prion can be maintained by the endogenous Ste18 protein (Table S9). However, mitotic stability of the [*STE*$^+$] was severely impaired after storage at -80^{o}C with subsequent recovery (Table S9). Similar to [*LSB*$^+$], [*STE*$^+$] isolates obtained in the *ssb1/2Δ* strain were not curable by GuHCl (Fig. 6E and Table S4), while [*PSI*$^+$] isolates

cross-seeded by [*STE*$^+$] were curable (Fig. S1 and Table S5). SDD-AGE analysis confirmed that [*STE*$^+$] isolates bearing the P_{CUP1}-*HA-STE18* construct and grown in the absence of extra Cu^{2+} contain a fraction of Ste18 protein in the form of detergent-resistant aggregates (Fig. 6F). Therefore, Ste18 aggregates behaved as heritable prions in the *ssb1/2Δ* background.

2.5 Effects of Ssb and Zuo1 on the [URE3] prion.

Previous data indicated that both deletion of genes coding for Hsp70-Ssb (*ssb1/2Δ*) and deletion of either RAC component (*ssz1Δ* or *zuo1Δ*) increase formation of the [*PSI*$^+$] prion [23, 26, 27, 30], while our new data (see above) show that *ssb1/2Δ* also promotes formation and heritability of the aggregated forms of Lsb2 and Ste18 proteins. However, it has been reported previously that *ssz1Δ* does not influence the formation of the prion form of yeast Ure2 protein, [*URE3*] [30]. Therefore, we have checked if *ssb1/2Δ* or *zuo1Δ* influence [*URE3*] formation. For this purpose, respective deletions were introduced into the yeast strain, bearing the reporter construct *DAL5::ADE2*, that allows the detection of [*URE3*] prion by growth on –Ade medium and lighter (white or pink versus red) color on complete YPD medium [39]. Fluctuation test data indicated that *ssb1/2Δ* did not influence, while *zuo1Δ* significantly increased both frequency (Fig. 7A and Table S10) and rate (5-fold, Fig. 7B and Table S10) of the formation of Ade$^+$ cells, compared to the isogenic WT strain. Notably, all strains preferentially produced Ade$^+$ colonies exhibiting mitotic loss of Ade$^+$ phenotypes at various levels compared to the *ssb1/2Δ* strain (Fig. 7, C and D, and Table S11). A majority of the Ade$^+$ colonies with high mitotic stability were curable by growth in the presence of GuHCl in all strains (Table S12). These data confirm that most Ade$^+$ isolates represent non-Mendelian elements (presumable [*URE3*] prions). Overall, our results show that *zuo1Δ* increases spontaneous formation of both unstable or curable (presumable [*URE3*] prions) and incurable (presumable mutants) Ade$^+$ derivatives, while *ssb1/2Δ* does not show a significant effect on [*URE3*] prion formation.

Next, we checked if the presence of Ssb influences the inheritance of [*URE3*] prions obtained in the *ssb1/2Δ* background. Such an effect was suggested by the observation that the *ssb1/2Δ* strain produced lower proportion of highly unstable spontaneous [*URE3*] isolates, compared to the WT and *zuo1Δ* strains (Fig. 7D and Table S11). To investigate the effect of Ssb on the [*URE3*] stability further, GuHCl-curable [*URE3*] isolates obtained in the *ssb1/2Δ* strain were transformed with a plasmid, expressing either *SSB1* from a strong constitutive P_{GPD} promoter, or *SSB2* from its endogenous promoter. Typically, the [*URE3*] prion was either completely lost (2 out of 9 isolates tested), or completely or partially inhibited and mitotically destabilized (remaining 7 isolates) after reintroduction of *SSB1* (see examples on Fig. 7E and data in Table S13). Reintroduction of *SSB2* completely or partially inhibited and mitotically destabilized [*URE3*] in 5

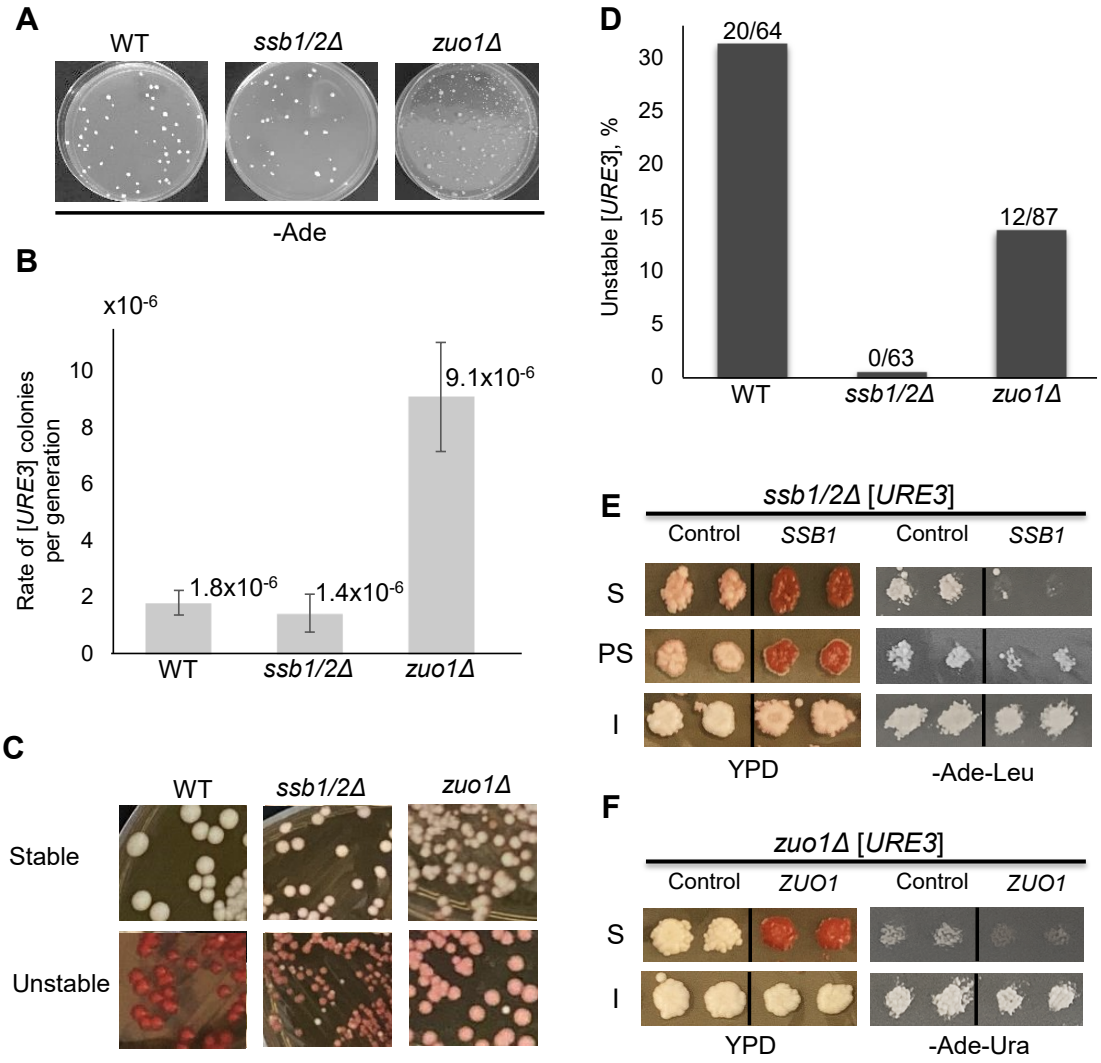

Figure 7. Effects of Ssb and Zuo1 proteins on the [*URE3*] prion. (A) Examples of -Ade plates with approximately equal amounts of cells plated, showing spontaneous formation of presumable [*URE3*] (Ade^+) colonies in the isogenic WT, *ssb1/2Δ* and *zuo1Δ* strains. (B) Rates of [*URE3*] formation in the isogenic WT, *ssb1/2Δ* and *zuo1Δ* strains, determined from fluctuation test. Error bars represent the 95% confidence limits. For frequencies and numbers, see Table S10. (C) Examples of mitotic stabilities of [*URE3*] prions arisen spontaneously in isogenic WT, *ssb1/2Δ* and *zuo1Δ* strains. In each case, an Ade^+ colony were streaked out for single subcolonies on YPD medium. The prion retention and loss were detected by respectively whitish and reddish color of subcolonies. (D) Distribution of unstable derivatives among the [*URE3*] isolates, arisen spontaneously in the WT, *ssb1/2Δ* and *zuo1Δ* strains. For more detailed information, see Table S11. (E) Inhibition of some [*URE3*] prions, obtained in the *ssb1/2Δ* background, by reintroduction of the plasmid bearing the *GFP-SSB1* construct (*SSB1*) under the control of strong constitutive glyceraldehyde-3-phosphate dehydrogenase promoter (P_{GDP}). The transformants were patched on the plasmid-selective medium (-Leu) and velveteen replica plated to YPD medium (for the color assay) and to –Ade-Leu medium (for the growth assay). Empty vector was used as a control. Similar results were obtained after reintroduction of the plasmid with *SSB2* gene under its endogenous promoter. For more detailed information, see Table S13. (F) Inhibition of some [*URE3*] prions, obtained in the *zuo1Δ* background, by reintroduction of the plasmid bearing the *ZUO1* gene under the control of strong constitutive EF1α (P_{TEF1}) promoter. The transformants were patched on the plasmid-selective medium (-Ura) and velveteen replica plated to YPD medium (for the color assay) and to –Ade-Ura medium (for the growth assay). For more detailed information, see Tables S14 and S15. Designations on panels E and F are as follows: S - sensitive, PS – partially sensitive, I – insensitive to reintroduction of Ssb (E) or Zuo1 (F).

out of 6 isolates tested (Table S13). Notably, introduction of the same *SSB1* or *SSB2* plasmids did not have any significant impact on the [*URE3*] isolates obtained in the WT strain, except somewhat increasing mitotic stability in one case (Table S13). This confirms that the inhibitory effect on [*URE3*] was primarily due to reintroduction of Ssb rather than due to its potential overexpression from a plasmid-based gene. Overall, these data show that while Ssb does not influence spontaneous formation of [*URE3*], it does significantly impair phenotypic expression and/or propagation of most [*URE3*] isolates.

Likewise, we checked if reintroduction of *ZUO1* influences the phenotypic manifestation of Ade^+ isolates obtained in the *zuo1Δ* background (Fig. 7F, and Table S14). In 2 out of 4 *zuo1Δ* Ade^+ isolates tested, growth on –Ade was completely inhibited, and color became more reddish in the presence of *ZUO1*, expressed from the strong constitutive P_{TEF1} promoter. Analysis of individual colonies obtained from these isolates confirmed that the [*URE3*] prion has been lost after introduction of the P_{TEF1}-*ZUO1* construct. No such destabilization of [*URE3*] occurred among

6 isolates obtained in the WT strain. Overall, our data show that at least some [*URE3*] prions obtained in the absence of Zuo1 are sensitive to the reintroduction of Zuo1, confirming the impact of a RAC component on the [*URE3*] prion.

2.6 Effects of Ssb on detection and mitotic stability of [PSI⁺].

While the effect of Ssb on the [*PSI*⁺] prion is well established, some discrepancies remained. For example, our previous data indicated that most of the *ssb1/2Δ*-derived [*PSI*⁺] isolates remain detectable after transformation with the *SSB1*-containing plasmid [23]. However, Son and Wickner reported that a significant fraction of [*PSI*⁺] isolates obtained in the *ssb1/2Δ* strain are not detectable after the mating to the strain bearing the wild type *SSB1* and *SSB2* alleles [30]. In

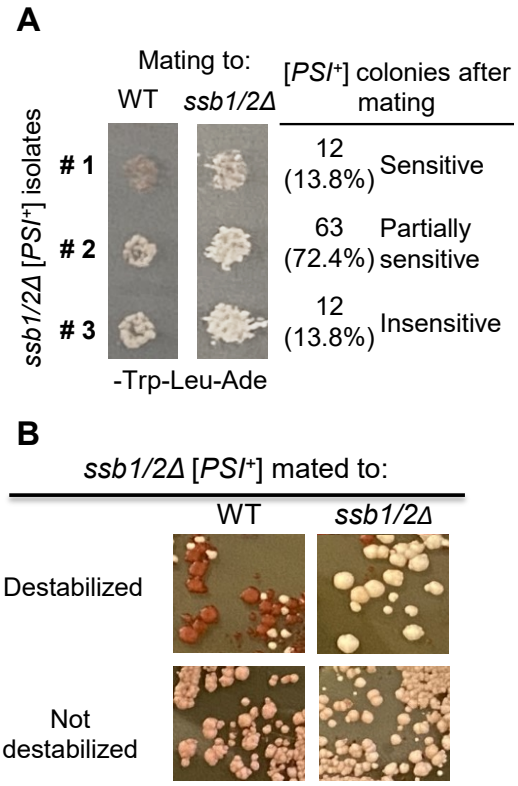

Figure 8. Effect of the reintroduction of Ssb on [*PSI*⁺] isolates obtained in the *ssb1/2Δ* background. (A) Independent *ssb1/2Δ* [*PSI*⁺] derivatives with *TRP1* plasmid were mated to isogenic WT and *ssb1/2Δ* strains of the opposite mating type (*MATα*) carrying a plasmid with the complementary (*LEU2*) marker. Resulting diploids were selected on –Trp-Leu medium and velveteen replica plated to the –Trp-Leu-Ade to detect the presence and stringency of [*PSI*⁺]. (B) Mitotic stability of [*PSI*⁺] prion in diploids obtained as described above for panel A. Diploids were streaked on appropriate selective media (-Trp-Ura) and velveteen replica plated to YPD for the color assay. Examples are shown; see text for numbers.

order to recheck the effect of Ssb reintroduction on [*PSI*$^+$] stability by using the approach similar to that of Son and Wickner, we mated a sample of [*PSI*$^+$] isolates, induced by transient overproduction of Sup35N in the [*psi*$^-$ *PIN*$^+$] *ssb1/2Δ* strain, to the [*pin*$^-$ *psi*$^-$] WT and *ssb1/2Δ* strains of the opposite mating type (*MAT*α). About 14% of the [*PSI*$^+$] isolates have lost suppression of *ade1-14* after mating, while another 72% exhibited lower suppression after mating to the WT strain, as compared to mating to *ssb1/2Δ* (Fig. 8A). Importantly, 5 (about 40%) out of 12 tested [*PSI*$^+$] isolates retaining prion exhibited decreased mitotic stability of a prion after reintroduction of Ssb (as judged from increased appearance of red, [*psi*$^-$] and mosaic, mixed [*PSI*$^+$]/[*psi*$^-$] subcolonies in their mitotic progeny), as compared to the mating to the *ssb1/2Δ* partner (Fig. 8B). Taken together, our data demonstrate that while reintroduction of Ssb indeed decreases phenotypic manifestation of most and mitotic stability of some [*PSI*$^+$] isolates obtained in the *ssb1/2Δ* background, majority (about 86%) of these [*PSI*$^+$] isolates remain detectable in the presence of Ssb, at least in the yeast strain used in our work.

3. Discussion

3.1 Comparison of the effects of ribosome-associated chaperones on [PSI$^+$] and other prions.

Previous reports by us [23, 27-29, 40] and others [24-26, 30] indicated that alterations of Ssb/RAC complex influence the Sup35 prion, [*PSI*$^+$]. However, the deletion of at least one gene coding for a RAC component, *SSZ1*, did not show an effect on another prion, [*URE3*] [30]. This led to the suggestion that the effects of ribosome-associated chaperones are specific to the prion form of Sup35, which is a translation factor, working in association with the ribosome. However, our new data show that the lack of Ssb influences heritable aggregation of several yeast proteins, namely Lsb2 (cytoskeleton-associated protein), Ste18 (Gγ subunit in the G-coupled receptor associate signaling pathway) and Ure2 (a regulator in nitrogen metabolism). These results clearly demonstrate that Hsp70-Ssb is a general modulator of heritable aggregation of a variety of proteins in the yeast cell, including those not related to the translational apparatus.

Patterns and specific features of the Ssb effects could vary depending on a target protein. In the case of Sup35, both an increase in *de novo* prion formation [23] and a promotion of prion propagation after stress [29] or in normal conditions [30] in the absence of Ssb have previously been reported. Son and Wickner [30] observed that most [*PSI*$^+$] prions obtained in the absence of Ssb are lost after reintroduction of Ssb by mating, suggesting that the impact of Ssb on detectable *de novo* [*PSI*$^+$] formation could be, in a significant part, due to the inability to detect the Ssb-sensitive prions in the WT strain. However, our experiments using the same approach as in the Son and Wickner paper indicate that while reintroduction of Ssb indeed partially inhibits or destabilizes a majority of [*PSI*$^+$] isolates generated in the *ssb1/2Δ* background, most of them remain phenotypically detectable in the Ssb$^+$ diploid (Fig. 8). This confirms our previous results obtained after reintroduction of *SSB1* on a plasmid [23], and supports our previous conclusion that Ssb has a dual effect on Sup35 prions, inhibiting both *de novo* prion formation and propagation of a pre-existing prion [27, 28]. This should be noted that despite numerical differences from our results, that are likely explained by different genotypic backgrounds of yeast strains and/or by using different inducer constructs, Son and Wickner calculations also agree with a notion of such a dual effect [30]. As argued in our previous work [27, 28], it is likely that the inhibitory effect of Ssb on *de novo* prion formation is due to promotion of the proper protein folding into a non-prion conformation by Ssb, while an inhibition of prion propagation could be explained by a competition between cytosolic Hsp70-Ssb and Hsp70-Ssa (involved in prion propagation) for binding to the Sup35 prion aggregates.

3.2 Formation and propagation of the [LSB$^+$] prion in the absence of Ssb.

In addition to the “classic” prions of [*PSI*$^+$] and [*URE3*], lack of Ssb increases *de novo* formation and promotes mitotic transmission of a typically metastable prion, formed by the cytoskeleton-associated protein Lsb2 (Figs. 1 and 2). While an effect of *ssb1/2Δ* on mitotic stability of [*LSB*$^+$] prion is dramatic, it is not likely that an increased observable formation of [*LSB*$^+$]

is solely due to improved mitotic transmission, because prion formation by the 8Q-8N mutant derivative of Lsb2, typically producing prions with high mitotic stability [10], is also increased in the *ssb1/2Δ* background (Fig. 3C). This shows that, like in case of [*PSI*$^+$], Ssb has a dual effect on both [*LSB*$^+$] prion formation and propagation.

Lsb2 is a short-lived stress-inducible protein, degraded via the UPS [31]. Levels of Lsb2 are increased in the *ssb1/2Δ* strain, compared to the WT strain. This increase is not solely due to the effect of *ssb1/2Δ* on *LSB2* transcription from its endogenous promoter, as it is observed with both endogenous (Fig. 1A) and artificial (P_{CUP1}, Fig. 1B and Fig. 3A-C) promoters. It is possible that the increase in Lsb2 levels in the absence of Ssb is at least in part due to the impact of *ssb1/2Δ* on ubiquitination-dependent degradation of Lsb2, however this question remains open, as the impact of ubiquitination site knockout on the Lsb2 levels is slight and not always reproducible (see Fig. 3, A and B). While an increase in Lsb2 levels could possibly contribute to an increase in prion formation and mitotic stability in the absence of Ssb, some results cannot be solely explained by this mechanism. Specifically, the mutant Lsb2-W91S derivative, that is not capable of binding actin cytoskeleton via Las17 and cannot produce a prion in the WT strain, acquires the prion properties in the *ssb1/2Δ* background and becomes capable of inducing [*LSB*$^+$] formation even at low protein levels, even though it can not do so at much higher levels in the Ssb$^+$ strain (Fig. 3, C and D).

Notably, the [*LSB*$^+$] prions, obtained and propagated in the *ssb1/2Δ* background are typically curable neither by GuHCl (Fig. 2C and Table S4), which is known to inhibit Hsp104 [35, 36], nor by transient inactivation or overproduction of Hsp104 (Fig. 2E). These data show that propagation of the [*LSB*$^+$] prion in the *ssb1/2Δ* background does not require Hsp104 activity at the level required for propagation of other yeast prions such as [*PSI*$^+$] or [*PIN*$^+$]. Further studies are needed to determine whether the absence of Ssb alters interactions between Hsp104 and [*LSB*$^+$] aggregates, or a different kind of [*LSB*$^+$] prion variants is preferentially produced in the *ssb1/2Δ*

background, compared to the Ssb$^+$ background. This should be noted that while previously we observed an increased loss of [*LSB*$^+$] in the presence of GuHCl in the WT strain [10], the interpretation of this result is somewhat ambiguous, because mitotic stability of [*LSB*$^+$] in the WT cells is very low even in the absence of GuHCl, so that systematic characterization of a variety of [*LSB*$^+$] isolates in regard to GuHCl-mediated curing was difficult. Therefore, it can not be excluded that a significant fraction of [*LSB*$^+$] isolates are not curable by GuHCl independently of the presence or absence of Ssb. Examples of yeast prions that are not dependent of Hsp104 are reported in literature [41-44], although most of such prions were shown to be of non-amyloid nature. While Lsb2 aggregates definitely possess some features of amyloids such as resistance to detergents (see Figs. 2B, 2D and 4E), it is possible that they are different from "typical" amyloids and that Hsp104 is not crucial for their fragmentation.

3.3 Role of Ssb in cellular memory.

Previously we reported that [*PSI*$^+$]-nucleating prions are induced in the Lsb2-dependent manner by heat stress, thus implicating metastable Lsb2 aggregates as carriers of cellular memory of stress [10, 45]. Notably, the lack of Ssb significantly increases accumulation of such prions, initially designated as [*PRN*$^+$] (Fig. 4, A and B, and Table S6). We have demonstrated that in majority of the cases, the [*PRN*$^+$] isolates indeed contain an aggregated form of Lsb2, implicating them as variants of [*LSB*$^+$] (Fig. 4E). Even a non-stressed exponentially growing *ssb1/2Δ* culture accumulated about 6% of [*PRN*$^+$] cells; after heat stress, their frequency was increased up to 17% (Fig. 4B). This result points to that Lsb2 is apparently a major yeast protein forming heritable aggregates in response to heat stress, while Ssb is a major chaperone downregulating formation and propagation of these aggregates. Biological meaning of this regulation could be explained by potentially adaptive effect of Lsb2 prion during stress as proposed in [45], coupled with its potentially detrimental impact on the non-stressed cells. Thus, Ssb could be responsible for keeping the fraction of the cells with stress-induced prions low,

457 diminishing prion interference with the efficient recovery and proliferation of the majority of the
458 culture after stress.

459 While mitotic stability of stress-induced [*LSB*$^{+}$] isolates was increased in the *ssb1/2Δ* strain,
460 compared to rare and highly unstable isolates detected in the WT strain (Fig. 4A and Table S3),
461 most heat-induced *ssb1/2Δ* [*LSB*$^{+}$] isolates were characterized by lower mitotic stability compared
462 to most *ssb1/2Δ* [*LSB*$^{+}$] isolates generated after artificial overproduction of Lsb2 (Table S3). This
463 shows that either heat stress preferentially produces different variants of the [*LSB*$^{+}$] prion,
464 compared to the prions induced by artificial Lsb2 overproduction, or simply the initially generated
465 fraction of aggregated Lsb2 protein is smaller after heat shock, compared to plasmid-mediated
466 overproduction of Lsb2. In the latter scenario, it is more difficult for the aggregated isoform to
467 efficiently overtake the whole protein pool in the cells, that explains its higher loss in subsequenrt
468 cell divisions.

469 Another yeast protein, a Gγ-subunit (Ste18), forms non-heritable detergent-resistant
470 aggregates upon overproduction in the WT strain [13]. These aggregates resemble “mnemons”
471 previously described for another yeast protein in the pheromone signaling pathway, Whi3 [12].
472 Notably, Ste18 aggregates are increased in abundance and become partly heritable in the
473 *ssb1/2Δ* strain (Figs. 5 and 6), indicating that the Ste18 mnemon is converted into a heritable
474 prion in the absence of Ssb. Like in the case of Lsb2, Ste18 is an unstable protein degraded via
475 the ubiquitin-proteasome system [13], and its levels are somewhat increased in the absence of
476 Ssb (Fig. 5A). However, this does not seem likely that such a relatively modest increase in levels
477 (at about 1.5-fold at high levels of Ste18 production, Fig. 5A) is sufficient to explain promotion of
478 both formation and heritability of Ste18 aggregates.

479 *3.4 Modulation of the [URE3] prion by ribosome-associated chaperones.*

480 In the case of the [*URE3*] prion, no effect of *ssb1/2Δ* on the rate of spontaneous prion

formation has been detected (Fig. 7 and Table S10). However, a larger proportion of mitotically unstable [*URE3*] variants has been recovered in the WT background, compared to the *ssb1/2Δ* strain (Fig. 7C and D, and Table S11). Moreover, reintroduction of the *SSB1* or *SSB2* gene on a plasmid led to the partial or complete inhibition of the phenotypic manifestation of vast majority of [*URE3*] isolates, generated in the *ssb1/2Δ* background (Fig. 7F and Table S13). As the [*URE3*] detection assay is not based on translational readthrough, this effect could not be due to the previously described effect of *ssb1/2Δ* on nonsense-suppression [23, 30], that is partially contributing to the inhibition of [*PSI*$^+$] by Ssb. More likely, inhibition of [*URE3*] occurred due to destabilization of some prion isolates in the presence of Ssb as shown in Table S14. The observation that partial inhibition of prion manifestation and mitotic transmission by Ssb does not result in significant differences in the frequencies and rates of detectable [*URE3*] formation between the WT and *ssb1/2Δ* strains (Fig. 7B and S4, and Table S10) provides an additional argument in favor of the notion that the effect of Ssb on the formation of other heritable aggregates ([*PSI*$^+$], [*LSB*$^+$] and [*STE*$^+$]) is not a simple consequence of the effects of Ssb on [*PSI*$^+$] manifestation and mitotic stability.

In contrast to *ssb1/2Δ*, deletion of the gene coding for the RAC component Zuo1 (an Hsp40 cochaperone of Hsp70-Ssb) led to a significant (5-fold) increase in the rate of the Ade$^+$ colonies detected by the [*URE3*] reporter system (Fig. 7A and B, and Table S10). Most of Ade$^+$ colonies were either mitotically unstable (Fig. 7C and D, and Table S11), or GuHCl-curable (Fig. 7E and Table S12), or both, implicating them as [*URE3*] prions. This shows that *zuo1Δ* increases spontaneous formation of the [*URE3*] prion, similar to the previously described effect of *zuo1Δ* on the formation of [*PSI*$^+$] prion. It should be noted that according to our previous data [27], *zuo1Δ* decreases mitotic stability of some [*PSI*$^+$] isolates in an Ssb-dependent manner. We suggested that this occurred due to relocation of Ssb from the ribosome to cytosol in *zuo1Δ* cells, as shown previously [46] and confirmed in our studies [27]. Cytosolic Ssb competes with Ssa involved in

[*PSI*$^{+}$] propagation [27, 28]. Likely the similar scenario could work in case of [*URE3*]. Notably, phenotypic manifestation and/or mitotic transmission of some [*URE3*] isolates obtained in the *zuo1Δ* background were inhibited by reintroduction of *ZUO1* gene (Fig. 7G). [*PSI*$^{+}$] isolates with such a sensitivity to RAC components have also been described [30, 47]. One possible explanation in case of [*URE3*] is that an increased level of at least one member of the Ssa family is known to destabilize the [*URE3*] prion [48], while increased accumulation of Ssb to the cytosol in the absence of *ZUO1* could partly compensate for this effect by antagonizing Ssa.

3.5 Biological relevance and future perspectives.

Our data implicate the ribosome-associated chaperoning machinery as a universal modulator of heritable protein aggregation in the yeast cell, as components of this machinery impact formation and propagation of prions formed by various proteins. Ssb consistently counteracts heritable protein aggregation, even though specifics of its effect on various aggregating proteins vary. This is consistent with the role of Ssb as one of the perpetuators of an anti-prion defense, as discussed previously [30]. An anti-prion activity of Ssb may employ various mutually non-exclusive mechanisms, including promoting the non-prion folding of nascent polypeptides, antagonizing accumulation of potentially aggregating proteins, and inhibiting the activity of the cytosolic chaperoning machinery that is involved in fragmentation and propagation of prion aggregates. Our previous data showing the modulation of the intracellular localization and prion-related activities of Ssb by environmental and physiological conditions [27-29] indicate that an anti-prion effect of Ssb is physiologically relevant and may provide a mechanism for the cross-talk between the protein biosynthesis machinery and self-perpetuating protein aggregation. This is also line with previously important increase of prion formation in yeast cells lacking multiple anti-prion proteins [47], and is further confirmed by our new results showing that Ssb influences aggregates involved in cellular memory. Overall physiological impact of Ssb-dependent modulation of heritable aggregation and cellular memory could be quite dramatic, as signified by

accumulation of a high proportion (up to 17%) of cells bearing the Lsb2 prion in the Ssb-deficient culture after heat stress (Fig. 4B).

While Hsp70-Ssb protein is specific to fungi, its RAC cochaperones are conserved from yeast to mammals, so that other member(s) of the Hsp70 family are playing the roles similar to Ssb in mammalian cells [49]. Indeed, human orthologs of Zuo1 and Ssz1 are shown to antagonize [*PSI*$^+$] formation in yeast cells lacking endogenous RAC [50]. Therefore, the relationship between the ribosome-associated chaperone machinery and self-perpetuating protein aggregation, established in our work, could likely be relevant beyond yeast and may contribute to both protein assembly disorders and biological effects of self-perpetuating protein aggregation in higher eukaryotes.

4. Materials and Methods

4.1 Yeast strains.

The *S. cerevisiae* strains used in this study are listed in Table S15. The isogenic haploid *MAT***a** [*psi*$^-$ *pin*$^-$] yeast strains with (GT1786, [27]) or without (GT409, [40]) the *ssb1/2Δ* deletion, and [*psi*$^-$ *PIN*$^+$] strains with (GT157) or without (GT159) the *ssb1/2Δ* deletion [23], derived from the GT81 series were described earlier. All [*LSB*$^+$], [*PRN*$^+$] and [*STE*$^+$] isolates were obtained in the [*psi*$^-$ *pin*$^-$] strains, while experiments checking the impact of *ssb1/2Δ* on the mitotic stability of newly formed *[PSI*$^+$] isolates were performed in the [*psi*$^-$ *PIN*$^+$] strains. The isogenic WT [*psi*$^-$ *pin*$^-$] strain of the opposite mating type, *MATα* (GT197) was described previously [40]. The isogenic [PSI+ PIN+] *MATα* strain GT1780-1D bearing *ssb1/2Δ* was constructed by D. Kiktev via mating haploid strains of the GT81 origin with *zuo1Δ::HIS3*, and with *ssb1Δ::HIS3* and *ssb2Δ::ura3* deletions, followed by sporulating and dissecting resulting diploid, and verifying deletion combinations in the spore clones by PCR. The [*psi*$^-$ *pin*$^-$] *MATα ssb1/2Δ* strain GT2340 was produced via curing the [*PSI*$^+$] and [*PIN*$^+$] prions from the strain GT1780-1D (described above) by GuHCl. The [*psi*$^-$ *pin*$^-$] *MATα*

555 strains were used in genetic crosses for reintroducing chaperones Ssb or Zuo1, or for introducing
556 plasmids overexpressing Hsp104 or producing dominant-negative derivative of Hsp104. WTY664
557 is an *lsb2Δ* derivative of the [*psi*$^-$ *pin*$^-$] strain GT409, constructed as described previously [31].
558 GT2383 is an *lsb2Δ* derivative of the [*psi*$^-$ *pin*-] *ssb1/2Δ* strain GT1786, constructed by replacing
559 the *LSB2* gene with bacterial *KanMX* gene, conferring resistance to G418 and PCR-amplified
560 from pFA6a-KanMX6 plasmid as in ref. [51]. The [*ure3-0*] strain BY241 [52] was kindly provided
561 by R. Wickner. The *zuo1Δ* (GT2175) derivative of BY241 was constructed by replacing *ZUO1*
562 gene with *KanMX* gene, as in ref. [51]. The *ssb1/2Δ* (GT2438) derivative of BY241 was
563 constructed by two subsequent replacements of the *SSB1* and *SSB2* genes respectively with
564 *TRP1* and *URA3* genes, PCR amplified from respective plasmids [51] using primers with
565 extensions homologous to flanking region of a respective gene.

566 *4.2 Plasmids.*

567 Basic centromeric *URA3* yeast vector pRS316 [53] was typically used as an empty control for
568 *URA3*-based plasmids. Centromeric *URA3* plasmids, bearing the WT or HA-tagged *LSB2*, mutant
569 derivatives of *HA-LSB2*, and the *LSB2-GFP* construct [10, 31, 54], or *HA-STE18* and *GFP-STE18*
570 constructs [13] under the control of copper-inducible P_{CUP1} promoter were described earlier. The
571 centromeric *TRP1* plasmid pFL39GAL-SUP35N [55], containing the region coding for the first 113
572 amino acid residues of Sup35N domain under the control of galactose-inducible P_{GAL} promoter
573 was used to induce [*PSI*$^+$] formation in the [*psi*$^-$] strains. Centromeric *URA3* plasmids pRS316-
574 TEF-SSB1 [40] and pRS416-TEF-ZUO1 [56], bearing the *SSB1* and *ZUO1* genes, respectively,
575 under the control of the translation elongation factor 1α promoter (P_{TEF}) were kindly provided by
576 E. Craig. Multicopy 2μ DNA based *LEU2* plasmid YEp351-GDP-GFP-SSB1, bearing the *GFP-*
577 *SSB1* construct under the P_{GPD} promoter, was created by cloning the *Sac*I-*Not*I fragment,
578 containing the chimeric *GFP-SSB1* ORF from the plasmid pRS316-GFP-SSB1 [57], kindly
579 provided by E. Deuerling, into the plasmid pRS316-GPD [58], cut with the same enzymes, and

580 then transferring the *Sal*I-*Sac*I fragment, containing the P_{GDP}-*GFP-SSB1* cassette from this
581 plasmid to YEp351 [59] cut with the same enzymes. Centromeric *LEU2* plasmid p366-SSB2,
582 bearing the *SSB2* gene under its own promoter, was identified by J. Patterson in Chernoff lab
583 from the p366-based yeast genomic library, kindly provided by P. Hieter. The centromeric
584 plasmids bearing the WT *HSP104* gene under the highly expressed P_{GPD} promoter and *LEU2*
585 marker, pLH105, or the dominant negative allele of *HSP104*, *HSP104-DN*, with double K218,620T
586 substitution inactivating both ATP-binding sites, and *URA3* marker [60] originated from the
587 laboratory of S. Lindquist and were based on pRS415 [53] and pRS316, respectively.

588 *4.3 Growth conditions and phenotype detection.*

589 The standard protocols were used for the preparation of the yeast complete organic (YPD) and
590 synthetic media, and for yeast transformation [61]. The synthetic yeast medium contained 3 μM
591 copper sulfate ($CuSO_4$); it was supplemented with 25 to 200 μM $CuSO_4$ (as indicated) in order to
592 increase expression of genes placed under the copper promoter (P_{CUP1}). Typically, 2% glucose
593 was used as a carbon source. However, 2% galactose was added instead of glucose to induce
594 genes placed under a galactose-inducible promoter (P_{GAL}). 5-fluoroorotic acid (5-FOA) was used
595 in screens to select against *URA3* plasmids where necessary [62]. Organic YPG medium
596 containing 3% glycerol instead of glucose was used for identifying respiratory-incompetent (Pet^-)
597 colonies, arising from mitochondrial DNA loss, either spontaneously or during transformation. Due
598 to their slow growth and inability to induce P_{GAL}, there colonies were hard to employ in some of
599 our assays, thus they were typically excluded from the analysis. Yeast cells were incubated at
600 30°C unless stated otherwise. 10- or 50-ml samples placed into Oakridge 25 ml round bottom
601 tubes or 250 ml Erlenmeyer flasks respectively were used to grow yeast cultures in the liquid
602 medium with shaking at 200 rpm. The optical density of growing yeast cultures was monitored at
603 600 nm (OD_{600}) using a Shimadzu UV-2450 spectrophotometer. The presence of [*PSI*$^+$] or [*URE3*]
604 were determined by growth on –Ade medium and lighter color on YPD medium, that originate

either from readthrough of the UGA reporter allele *ade1-14* [4] or from induction of the [*URE3*]-dependent P_{DAL5}-*ADE2* reporter construct [39], respectively. This should be noted that non-prion ([*psi*$^-$] or [*ure3-0*]) Ade$^-$ strains with *ssb1/2Δ* or *zuo1Δ* deletions typically exhibit somewhat lighter color on YPD medium, compared to their Ssb$^+$ and Zuo$^+$ counterparts. This phenomenon is apparently due to partly impaired accumulation of red pigment in the Ssb- or RAC-deficient strains, however it does not prevent the color differentiation between the non-prion and prion cultures in respective backgrounds. The presence of [*LSB*$^+$] or [*STE*$^+$] was detected phenotypically by their ability to promote *de novo* formation of [*PSI*$^+$] after transient overproduction of Sup35N [10, 13]. For this purpose, the cultures bearing the *ade1-14* (UGA) reporter and plasmid pFL39GAL-SUP35N were incubated on the galactose medium selective for the plasmid, where the P_{GAL}-*SUP35N* construct is induced, and then velveteen replica plated onto the glucose –Ade medium for [*PSI*$^+$] detection. Excess Sup35N efficiently induces [*PSI*$^+$] formation only in the presence of other protein aggregates [4]. To assess prion curing by guanidine hydrochloride (GuHCl), an inhibitor of the chaperone Hsp104 [35, 63], yeast cultures were grown in parallel on the solid YPD medium and on YPD containing 5 mM (for the WT strains) or 2 mM (for the *ssb1/2Δ* or *zuo1Δ* strains that are hypersensitive to GuHCl) of GuHCl for three passages (typically 20-40 generations), following by streak outs on the medium lacking GuHCl and testing individual subcolonies (usually at least 8 or more from each original culture) for the presence of a respective prion by using the phenotypic assays described above.

4.4 Spontaneous formation of the [URE3] prion.

To measure the frequencies and rates of the spontaneous formation of [*URE3*], a fluctuation assay was performed in the same way as described previously for [*PSI*$^+$] [23]. No less than 12 independent cultures were analyzed for each strain. The frequency of Ade$^+$ colonies has been calculated as the ratio of Ade$^+$ colonies to the total number of colony forming units (viable cells) plated. The rate (R) of Ade$^+$ colonies (reflecting the rate of spontaneous [*URE3*] formation) was

630 calculated according to the formula $R=f/ln(NR)$, where f is the observed frequency of Ade$^+$
631 colonies, and N is the number of cells in the culture. Median rates and 95% confidence limits were
632 determined according to standard formulas [64]. To confirm that the majority of Ade$^+$ colonies
633 indeed originated from prion formation rather than from chromosomal mutation, tests for mitotic
634 stability and curing by GuHCl were performed.

635 *4.5 Prion induction by heat shock.*

636 To monitor the formation of prions with [*PSI*$^+$]-inducing capabilities during mild heat stress,
637 the WT and *ssb1/2Δ* [*pin*$^-$ *psi*$^-$] yeast strains bearing a plasmid with the P_{GAL}-*SUP35N TRP1*
638 construct were grown in the liquid YPD medium overnight at 25°C, inoculated into fresh YPD with
639 starting OD_{600} at about 0.1, and incubated for 2 hrs at 25°C with shaking at 200 rpm, followed by
640 incubation for 2 hrs at 39°C. The samples taken before and after 39°C treatment were plated onto
641 the glucose medium selective for the plasmid (-Trp), at the density of 200-300 cells per plate, and
642 grown at 25°C for 3-7 days. Grown colonies were velveteen replica plated to the same medium
643 with glucose (-Trp) or with galactose (-Trp+Gal) and incubated for 2 days, followed by velveteen
644 replica plating to –Ade medium. Colonies that produced growth or extensive papillation on -Ade
645 media after –Trp+Gal (but not after –Trp) were considered as prion-containing colonies, capable
646 of [*PSI*$^+$] induction after Sup35N overproduction. A subset of Ade$^+$ subcolonies were passaged on
647 GuHCl to check for curability, thus confirming that growth on –Ade was indeed due to the
648 formation of [*PSI*$^+$] prion.

649 *4.6 Mating assays for [LSB$^+$] retention.*

650 To check the effects of Hsp104 inactivation or overproduction on [*LSB*$^+$] prions in the
651 absence of Ssb, the *ssb1/2Δ* [*LSB*$^+$] isolates that have lost the P_{CUP1}-*HA-LSB2* plasmid but
652 retained the *TRP1* P_{GAL}-*SUP35N* construct and control *ssb1/2Δ* [*lsb*$^-$] isolates bearing P_{GAL}-
653 *SUP35N* were mated to the *ssb1/2Δ* [*lsb*$^-$] strain of opposite mating type, bearing the following
654 *URA3* plasmids: empty vector, dominant negative allele of *HSP104* (*HSP104-DN*), or *WT HSP104*

overexpressor cassette under the P_{GPD} promoter. In order to check the effects of Ssb reintroduction on [*LSB*$^+$] prions obtained in the absence of Ssb, both *MAT**a** ssb1/2Δ* [*LSB*$^+$] isolates that have lost the P_{CUP1}*-HA-LSB2* plasmid but retained the *TRP1* P_{GAL}*-SUP35N* construct, and control *ssb1/2Δ* [*lsb*$^-$] isolates bearing P_{GAL}*-SUP35N* were mated either to isogenic *MATα* [*psi*$^-$ *pin*$^-$ *lsb*$^-$] *Ssb*$^+$ strain, or to isogenic *MATα* [*psi*$^-$ *pin*$^-$ *lsb*$^-$] *ssb1/2Δ* strain of carrying either control *URA3* vector or *URA3* plasmid with constitutively expressed P_{TEF}*-SSB1* construct. For all selected diploids containing *URA3* plasmids, these plasmids were cured by counterselection on 5-FOA medium. Then, Sup35N was induced on galactose medium, followed by detection of [*LSB*$^+$] prion via its ability to cross-seed the formation of [*PSI*$^+$] prion, as seen on –Ade medium.

4.7 Protein analysis.

For protein isolation, yeast cells were collected by centrifugation at 3000 rpm for 5 min at 4°C, resuspended in 100-300 µl of ice-cold lysis buffer (25 mM Tris pH 7.5, 0.1M NaCl, 10 mM EDTA, 100 µg/ml cycloheximide, 2 mM benzamidine, 20 µg/ml leupeptin, 4 µg/ml pepstatin A, 1 mM N-ethylmaleimide, 1X protease inhibitor cocktail from Roche Diagnostics, 2 mM PMSF), mixed with ¼ (volume/volume) of 150-212 µM acid-washed glass beads from Sigma (catalog # G1145) and disrupted by vortexing at 4°C for 6 min. After removing cell debris by centrifugation at 5,900 g for 2 min, the supernatant was transferred to a clean microcentrifuge tube, and protein concentrations were measured using the colorimetric Bradford protein assay (BIO-RAD) [65]. Proteins were fractionated by sodium dodecyl sulfate - polyacrylamide gel electrophoresis (SDS-PAGE), and identified by Western blotting analysis followed by reaction to respective antibodies. For identification of detergent-resistant protein aggregates, either “boiled gel” SDS-PAGE or semi-denaturing detergent-agarose gel electrophoresis (SDD-AGE) were employed [34, 66]. In a “boiled gel” assay, SDS-containing protein samples (either pre-boiled as a control, or not pre-boiled) are run on the SDS-PAGE gel for about 1 hr, followed by interrupting electrophoresis, sealing wells with additional polyacrylamide, and “boiling” the whole gel within the plastic bag in

680 the steamed water bath for 10 min. After boiling, the gel is placed into the electrophoretic
681 apparatus, and electrophoresis is resumed. Detergent-resistant prion polymers are unable to
682 enter the SDS-PAGE without boiling, however they are solubilized and are entering the gel after
683 boiling. In SDD-AGE, aggregates and monomers from a sample containing a detergent (either
684 3% sodium N-lauroylsarkosine or 2% SDS) are separated by electrophoresis in the agarose gel
685 with buffer, containing 0.1% SDS, roughly in accordance with their sizes. After reaction to primary
686 and respective secondary antibodies, proteins were visualized using the chemiluminescent
687 detection reagent as described in the GE Healthcare protocol. Rabbit polyclonal antibodies to
688 Ade2, Ssb and Rnq1 were kindly provided by Dr. V. Alenin, Dr. E. Craig, and Dr. S. Lindquist,
689 respectively. Rabbit antibodies to HA (C29F4) and G6PDH (catalog # A9521) were from Cell
690 Signaling Technology, Danvers, MA, and Sigma-Aldrich, respectively. Rabbit antibodies
691 recognizing both Lsb1 and Lsb2 were generated by ProSci, Inc. (Poway, CA) and described
692 previously [31]. These antibodies recognize Lsb2 and both full-length and heat-shock induced
693 proteolytically processed (shortened) forms of its paralog Lsb1 [54]. Densitometry was performed
694 by using the program ImageJ, downloaded from https://imagej.nih.gov. Levels of proteins
695 measured (such Lsb2 and its derivatives, and Ste18) were always normalized by either Ade2 or
696 G6PDH, used as loading controls.

697 *4.8 Fluorescence microscopy.*

698 To visualize protein aggregates formed by Lsb2 or Ste18 *in vivo*, these proteins were tagged
699 by the green fluorescent protein (GFP) fluorophore. Cultures of strains bearing the *LSB2-GFP* or
700 *GFP-STE18* cassette on a plasmid under the control of copper-inducible (P_{CUP1}) promoter were
701 grown overnight in the liquid media selective for a plasmid (-Ura) and inoculated each into 10 ml
702 of the same fresh medium either not-containing or containing extra $CuSO_4$ (as specified on
703 Figures), with the starting OD_{600} of 0.4. 500-µl aliquots were taken from each culture at specified
704 time points; cells were spun down at 3,500 rpm for 2 min, then 10 µl aliquot of each sample was

taken from the bottom of the tube, placed onto a microscope slide with cover slip, and sealed with clear nail polish to prevent from drying. Fluorescence was monitored using a BX41 microscope (Olympus) at 100X (oil immersion) with the endow GFP bandpass emission (green) filter. Images were taken using an Olympus DP-71 camera.

5. Conclusions

Our data demonstrate that the ribosome-associated chaperone Hsp70-Ssb antagonizes formation and/or heritability of prion aggregates formed by a variety of yeast proteins, such as Lsb2, Ste18 and Ure2 (in addition to Sup35, for which this effect has been demonstrated previously). The Hsp40 cochaperone of Ssb, Zuo1 also influences formation and propagation of the prion form of Ure2. Almost 20% of the cells form a detectable prion after the mild heat stress in yeast culture lacking Ssb. Majority of these stress-induced prions represent a prion form of the Lsb2 protein. These results implicate Hsp70-Ssb as a major modulator of heritable protein aggregation and stress memory with a broad spectrum of action.

Supplemental Information

Supplemental Figures

Supplemental Tables

Author Contributions:

Conceptualization, Yury Chernoff; Formal analysis, Lina Jay-Garcia, Joseph Cornell, Rebecca Howie, Tatiana Chernova and Yury Chernoff; Funding acquisition, Yury Chernoff; Investigation, Lina Jay-Garcia, Joseph Cornell, Rebecca Howie, Quincy Faber and Abigail Salas; Resources, Tatiana Chernova; Supervision, Yury Chernoff; Writing - original draft, Lina Jay-Garcia and Yury Chernoff; Writing – review & editing, Lina Jay-Garcia, Joseph Cornell and Yury Chernoff. All authors have read and agreed to the published version of the manuscript.

Acknowledgements: This work was supported by the grant MCB 1817976 from the National Science Foundation. We thank Drs. V. Alenin, E. Craig, E. Deuerling, P. Hieter, S. Lindquist, M. Torres, J. Warner and R. Wickner for yeast strains, plasmids and antibodies, and Drs. D. Kiktev and J. Patterson for the help in some strain and/or DNA constructions.

Conflicts of Interest: The authors have nothing to disclose.

References

1. Prusiner SB: **Biology and genetics of prions causing neurodegeneration**. *Annu Rev Genet* 2013, **47**:601-623.
2. Tarutani A, Hasegawa M: **Prion-like propagation of alpha-synuclein in neurodegenerative diseases**. *Progress in molecular biology and translational science* 2019, **168**:323-348.
3. Walker LC, Jucker M: **Neurodegenerative diseases: expanding the prion concept**. *Annu Rev Neurosci* 2015, **38**:87-103.
4. Liebman SW, Chernoff YO: **Prions in yeast**. *Genetics* 2012, **191**(4):1041-1072.
5. Wickner RB, Edskes HK, Gorkovskiy A, Bezsonov EE, Stroobant EE: **Yeast and Fungal Prions: Amyloid-Handling Systems, Amyloid Structure, and Prion Biology**. *Adv Genet* 2016, **93**:191-236.
6. Chernoff YO, Grizel AV, Rubel AA, Zelinsky AA, Chandramowlishwaran P, Chernova TA: **Application of yeast to studying amyloid and prion diseases**. *Adv Genet* 2020, **105**:293-380.
7. McGlinchey RP, Kryndushkin D, Wickner RB: **Suicidal [PSI+] is a lethal yeast prion**. *Proc Natl Acad Sci U S A* 2011, **108**(13):5337-5341.
8. Nakayashiki T, Kurtzman CP, Edskes HK, Wickner RB: **Yeast prions [URE3] and [PSI+] are diseases**. *Proc Natl Acad Sci U S A* 2005, **102**(30):10575-10580.
9. Halfmann R, Lindquist S: **Epigenetics in the extreme: prions and the inheritance of environmentally acquired traits**. *Science* 2010, **330**(6004):629-632.
10. Chernova TA, Kiktev DA, Romanyuk AV, Shanks JR, Laur O, Ali M, Ghosh A, Kim D, Yang Z, Mang M *et al*: **Yeast Short-Lived Actin-Associated Protein Forms a Metastable Prion in Response to Thermal Stress**. *Cell reports* 2017, **18**(3):751-761.
11. Caudron F, Barral Y: **Mnemons: encoding memory by protein super-assembly**. *Microbial cell (Graz, Austria)* 2014, **1**(3):100-102.
12. Caudron F, Barral Y: **A super-assembly of Whi3 encodes memory of deceptive encounters by single cells during yeast courtship**. *Cell* 2013, **155**(6):1244-1257.
13. Chernova TA, Yang Z, Karpova TS, Shanks JR, Shcherbik N, Wilkinson KD, Chernoff YO: **Aggregation and Prion-Inducing Properties of the G-Protein Gamma Subunit Ste18 are Regulated by Membrane Association**. *Int J Mol Sci* 2020, **21**(14):5038.
14. Chernova TA, Wilkinson KD, Chernoff YO: **Prions, Chaperones, and Proteostasis in Yeast**. *Cold Spring Harb Perspect Biol* 2017, **9**(2):a023663
15. Winkler J, Tyedmers J, Bukau B, Mogk A: **Hsp70 targets Hsp100 chaperones to substrates for protein disaggregation and prion fragmentation**. *J Cell Biol* 2012, **198**(3):387-404.
16. Nakagawa Y, Shen HC, Komi Y, Sugiyama S, Kurinomaru T, Tomabechi Y, Krayukhina E, Okamoto K, Yokoyama T, Shirouzu M *et al*: **Amyloid conformation-dependent disaggregation in a reconstituted yeast prion system**. *Nat Chem Biol* 2022, **18**(3):321-331.
17. Matveenko AG, Barbitoff YA, Jay-Garcia LM, Chernoff YO, Zhouravleva GA: **Differential effects of chaperones on yeast prions: CURrent view**. *Curr Genet* 2018, **64**(2):317-325.
18. Gong Y, Kakihara Y, Krogan N, Greenblatt J, Emili A, Zhang Z, Houry WA: **An atlas of chaperone-protein interactions in Saccharomyces cerevisiae: implications to protein folding pathways in the cell**. *Mol Syst Biol* 2009, **5**:275.
19. Gautschi M, Lilie H, Funfschilling U, Mun A, Ross S, Lithgow T, Rucknagel P, Rospert S: **RAC, a stable ribosome-associated complex in yeast formed by the DnaK-DnaJ homologs Ssz1p and zuotin**. *Proc Natl Acad Sci U S A* 2001, **98**(7):3762-3767.

20. Gautschi M, Mun A, Ross S, Rospert S: **A functional chaperone triad on the yeast ribosome**. *Proc Natl Acad Sci USA* 2002, **99**(7):4209-4214.
21. Ghosh A, Shcherbik N: **Cooperativity between the Ribosome-Associated Chaperone Ssb/RAC and the Ubiquitin Ligase Ltn1 in Ubiquitination of Nascent Polypeptides**. *Int J Mol Sci* 2020, **21**(18):6815.
22. Nelson RJ, Ziegelhoffer T, Nicolet C, Werner-Washburne M, Craig EA: **The translation machinery and 70 kd heat shock protein cooperate in protein synthesis**. *Cell* 1992, **71**(1):97-105.
23. Chernoff YO, Newnam GP, Kumar J, Allen K, Zink AD: **Evidence for a protein mutator in yeast: role of the Hsp70-related chaperone ssb in formation, stability, and toxicity of the [PSI] prion**. *Mol Cell Biol* 1999, **19**(12):8103-8112.
24. Kushnirov VV, Kryndushkin DS, Boguta M, Smirnov VN, Ter-Avanesyan MD: **Chaperones that cure yeast artificial [PSI+] and their prion-specific effects**. *Curr Biol* 2000, **10**(22):1443-1446.
25. Chacinska A, Szczesniak B, Kochneva-Pervukhova NV, Kushnirov VV, Ter-Avanesyan MD, Boguta M: **Ssb1 chaperone is a [PSI+] prion-curing factor**. *Curr Genet* 2001, **39**(2):62-67.
26. Amor AJ, Castanzo DT, Delany SP, Selechnik DM, van Ooy A, Cameron DM: **The ribosome-associated complex antagonizes prion formation in yeast**. *Prion* 2015:0.
27. Kiktev DA, Melomed MM, Lu CD, Newnam GP, Chernoff YO: **Feedback control of prion formation and propagation by the ribosome-associated chaperone complex**. *Mol Microbiol* 2015, **96**(3):621-632.
28. Chernoff YO, Kiktev DA: **Dual role of ribosome-associated chaperones in prion formation and propagation**. *Current genetics* 2016, **62**(4):677-685.
29. Howie RL, Jay-Garcia LM, Kiktev DA, Faber QL, Murphy M, Rees KA, Sachwani N, Chernoff YO: **Role of the Cell Asymmetry Apparatus and Ribosome-Associated Chaperones in the Destabilization of a Saccharomyces cerevisiae Prion by Heat Shock**. *Genetics* 2019, **212**(3):757-771.
30. Son M, Wickner RB: **Normal levels of ribosome-associated chaperones cure two groups of [PSI+] prion variants**. *Proc Natl Acad Sci USA* 2020, **117**(42):26298-26306.
31. Chernova TA, Romanyuk AV, Karpova TS, Shanks JR, Ali M, Moffatt N, Howie RL, O'Dell A, McNally JG, Liebman SW *et al*: **Prion induction by the short-lived, stress-induced protein Lsb2 is regulated by ubiquitination and association with the actin cytoskeleton**. *Mol Cell* 2011, **43**(2):242-252.
32. Derkatch IL, Bradley ME, Zhou P, Chernoff YO, Liebman SW: **Genetic and environmental factors affecting the de novo appearance of the [PSI+] prion in Saccharomyces cerevisiae**. *Genetics* 1997, **147**(2):507-519.
33. Derkatch IL, Bradley ME, Hong JY, Liebman SW: **Prions affect the appearance of other prions: the story of [PIN(+)]**. *Cell* 2001, **106**(2):171-182.
34. Bagriantsev SN, Kushnirov VV, Liebman SW: **Analysis of amyloid aggregates using agarose gel electrophoresis**. *Methods Enzymol* 2006, **412**:33-48.
35. Ferreira PC, Ness F, Edwards SR, Cox BS, Tuite MF: **The elimination of the yeast [PSI+] prion by guanidine hydrochloride is the result of Hsp104 inactivation**. *Mol Microbiol* 2001, **40**(6):1357-1369.
36. Jung G, Jones G, Masison DC: **Amino acid residue 184 of yeast Hsp104 chaperone is critical for prion-curing by guanidine, prion propagation, and thermotolerance**. *Proc Natl Acad Sci U S A* 2002, **99**(15):9936-9941.
37. Corder GW, Foreman DI: **Nonparametric statistics: a step-by-step approach**. In: Second edition. edn. Hoboken, New Jersey: John Wiley & Sons,; 2014: ISBN 9781118840429.

38. Kushnirov VV, Alexandrov IM, Mitkevich OV, Shkundina IS, Ter-Avanesyan MD: **Purification and analysis of prion and amyloid aggregates**. *Methods* 2006, **39**(1):50-55.
39. Schlumpberger M, Prusiner SB, Herskowitz I: **Induction of distinct [URE3] yeast prion strains**. *Mol Cell Biol* 2001, **21**(20):7035-7046.
40. Allen KD, Wegrzyn RD, Chernova TA, Muller S, Newnam GP, Winslett PA, Wittich KB, Wilkinson KD, Chernoff YO: **Hsp70 chaperones as modulators of prion life cycle: novel effects of Ssa and Ssb on the Saccharomyces cerevisiae prion [PSI+]**. *Genetics* 2005, **169**(3):1227-1242.
41. Jarosz DF, Lancaster AK, Brown JC, Lindquist S: **An evolutionarily conserved prion-like element converts wild fungi from metabolic specialists to generalists**. *Cell* 2014, **158**(5):1072-1082.
42. Harvey ZH, Chakravarty AK, Futia RA, Jarosz DF: **A Prion Epigenetic Switch Establishes an Active Chromatin State**. *Cell* 2020, **180**(5):928-940 e914.
43. Chakravarty AK, Smejkal T, Itakura AK, Garcia DM, Jarosz DF: **A Non-amyloid Prion Particle that Activates a Heritable Gene Expression Program**. *Mol Cell* 2020, **77**(2):251-265 e259.
44. Garcia DM, Campbell EA, Jakobson CM, Tsuchiya M, Shaw EA, DiNardo AL, Kaeberlein M, Jarosz DF: **A prion accelerates proliferation at the expense of lifespan**. *eLife* 2021, **10:**e60917.
45. Chernova TA, Chernoff YO, Wilkinson KD: **Prion-based memory of heat stress in yeast**. *Prion* 2017, **11**(3):151-161.
46. Willmund F, del Alamo M, Pechmann S, Chen T, Albanese V, Dammer EB, Peng J, Frydman J: **The cotranslational function of ribosome-associated Hsp70 in eukaryotic protein homeostasis**. *Cell* 2013, **152**(1-2):196-209.
47. Son M, Wickner RB: **Antiprion systems in yeast cooperate to cure or prevent the generation of nearly all [PSI(+)] and [URE3] prions**. *Proc Natl Acad Sci U S A* 2022, **119**(28):e2205500119.
48. Schwimmer C, Masison DC: **Antagonistic interactions between yeast [PSI(+)] and [URE3] prions and curing of [URE3] by Hsp70 protein chaperone Ssa1p but not by Ssa2p**. *Mol Cell Biol* 2002, **22**(11):3590-3598.
49. Jaiswal H, Conz C, Otto H, Wolfle T, Fitzke E, Mayer MP, Rospert S: **The chaperone network connected to human ribosome-associated complex**. *Mol Cell Biol* 2011, **31**(6):1160-1173.
50. Kelly C, Ahmed Y, Elghawy O, Pachon NF, Fontanese MS, Kim S, Kitterman E, Marley A, Terrenzio D, Wike R *et al*: **The human ribosome-associated complex suppresses prion formation in yeast**. *Proteins* 2023.
51. Longtine MS MAr, Demarini DJ, Shah NG, Wach A, Brachat A, Philippsen P, Pringle JR.: **Additional modules for versatile and economical PCR-based gene deletion and modification in S cerevisiae.** . *Yeast* 1998, **14**:953-961.
52. Brachmann A, Baxa U, Wickner RB: **Prion generation in vitro: amyloid of Ure2p is infectious**. *EMBO J* 2005, **24**(17):3082-3092.
53. Sikorski RS, Hieter P: **A system of shuttle vectors and yeast host strains designed for efficient manipulation of DNA in Saccharomyces cerevisiae**. *Genetics* 1989, **122**(1):19-27.
54. Ali M, Chernova TA, Newnam GP, Yin L, Shanks J, Karpova TS, Lee A, Laur O, Subramanian S, Kim D *et al*: **Stress-dependent proteolytic processing of the actin assembly protein Lsb1 modulates a yeast prion**. *J Biol Chem* 2014, **289**(40):27625-27639.

55. Borchsenius AS, Wegrzyn RD, Newnam GP, Inge-Vechtomov SG, Chernoff YO: **Yeast prion protein derivative defective in aggregate shearing and production of new 'seeds'**. *EMBO J* 2001, **20**(23):6683-6691.
56. Meyer AE, Hung NJ, Yang P, Johnson AW, Craig EA: **The specialized cytosolic J-protein, Jjj1, functions in 60S ribosomal subunit biogenesis**. *Proc Natl Acad Sci USA* 2007, **104**(5):1558-1563.
57. Hanebuth MA, Kityk R, Fries SJ, Jain A, Kriel A, Albanese V, Frickey T, Peter C, Mayer MP, Frydman J *et al*: **Multivalent contacts of the Hsp70 Ssb contribute to its architecture on ribosomes and nascent chain interaction**. *Nature communications* 2016, **7**.
58. Li L, Lindquist S: **Creating a protein-based element of inheritance**. *Science* 2000, **287**(5453):661-664.
59. Hill JE, Myers AM, Koerner TJ, Tzagoloff A: **Yeast/E. coli shuttle vectors with multiple unique restriction sites**. *Yeast* 1986, **2**(3):163-167.
60. Chernoff YO, Lindquist SL, Ono B, Inge-Vechtomov SG, Liebman SW: **Role of the chaperone protein Hsp104 in propagation of the yeast prion-like factor [psi+]**. *Science* 1995, **268**(5212):880-884.
61. Sherman F: **Getting started with yeast**. *Methods Enzymol* 2002, **350**:3-41.
62. Boeke JD, LaCroute F, Fink GR: **A positive selection for mutants lacking orotidine-5'-phosphate decarboxylase activity in yeast: 5-fluoro-orotic acid resistance**. *Mol Gen Genet* 1984, **197**(2):345-346.
63. Hung GC, Masison DC: **N-terminal domain of yeast Hsp104 chaperone is dispensable for thermotolerance and prion propagation but necessary for curing prions by Hsp104 overexpression**. *Genetics* 2006, **173**(2):611-620.
64. Drake JW: **A constant rate of spontaneous mutation in DNA-based microbes**. *Proc Natl Acad Sci U S A* 1991, **88**(16):7160-7164.
65. Bradford MM: **A rapid and sensitive method for the quantitation of microgram quantities of protein utilizing the principle of protein-dye binding**. *Anal Biochem* 1976, **72**:248-254.
66. Drozdova PB, Barbitoff YA, Belousov MV, Skitchenko RK, Rogoza TM, Leclercq JY, Kajava AV, Matveenko AG, Zhouravleva GA, Bondarev SA: **Estimation of amyloid aggregate sizes with semi-denaturing detergent agarose gel electrophoresis and its limitations**. *Prion* 2020, **14**(1):118-128.